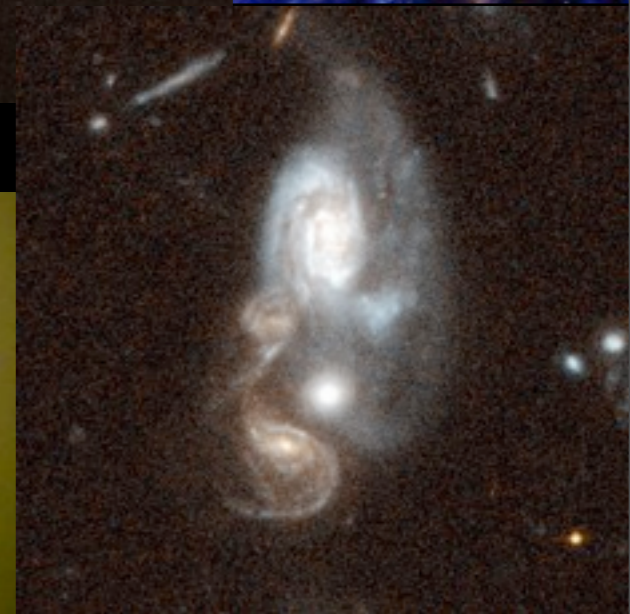


The View from 5AU
March 25-26, 2010

EBL with GRB and Blazars

Joel Primack

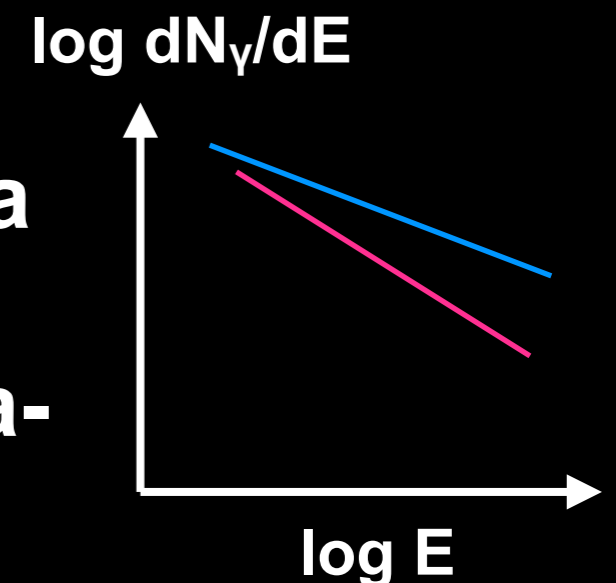
with Rudy Gilmore, Alberto Dominguez, & Rachel Somerville



The EBL is very difficult to observe directly because of foregrounds, especially the zodiacal light. Reliable lower limits are obtained by integrating the light from observed galaxies. The best upper limits come from (non-) attenuation of gamma rays from distant blazars, but these are uncertain because of the unknown emitted spectrum of these blazars.

This talk concerns both the **optical-IR** EBL relevant to attenuation of TeV gamma rays, and also the **UV EBL** relevant to attenuation of gamma rays from very distant sources observed by *Fermi* and low-threshold ground-based ACTs.

Just as IR light penetrates dust better than shorter wavelengths, so lower energy gamma rays penetrate the EBL better than higher energy, resulting in a **softer** observed gamma-ray spectrum from more distant sources.



PILLAR OF STAR BIRTH
Carina Nebula in UV Visible Light



WFC3/UVIS

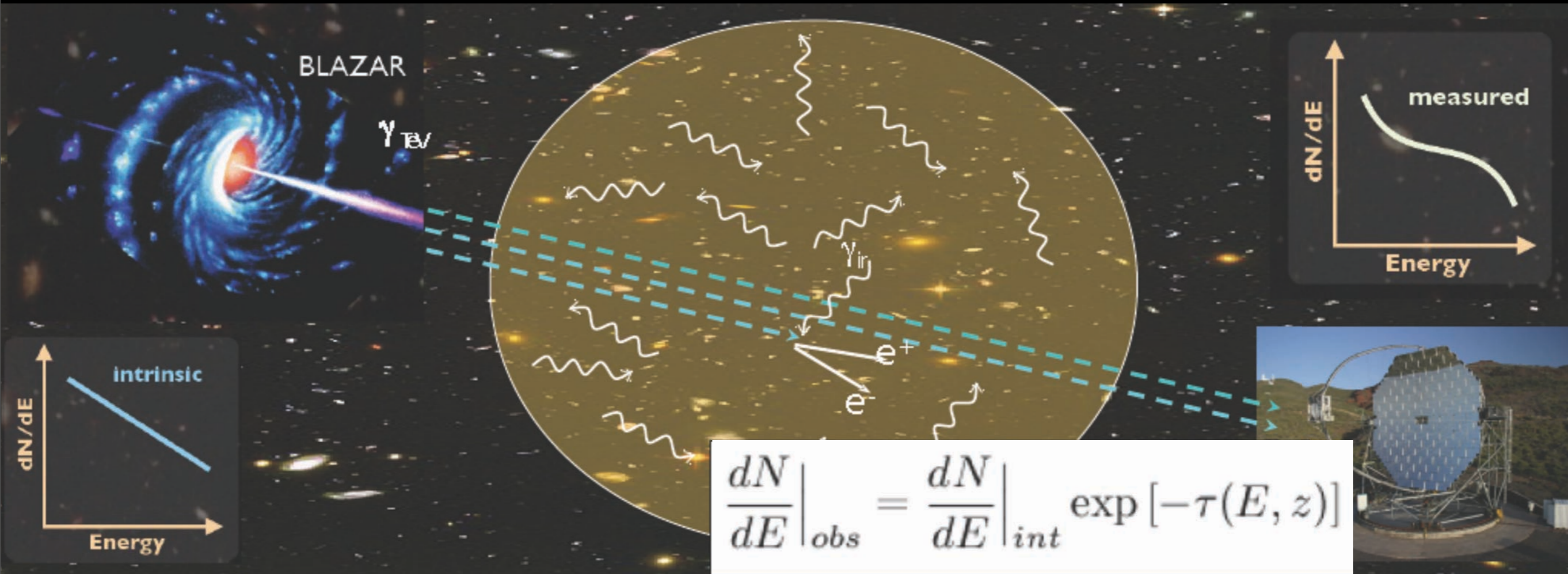
PILLAR OF STAR BIRTH
Carina Nebula in IR Light

**Longer wavelength light
penetrates the dust better**

**Longer wavelength gamma rays
also penetrate the EBL better**

WFC3/IR

Gamma Ray Attenuation due to $\gamma\gamma \rightarrow e^+e^-$



If we know the intrinsic spectrum, we can infer the optical depth $\tau(E, z)$ from the observed spectrum. In practice, we **assume** that $\frac{dN}{dE} \Big|_{int}$ is not harder than $E^{-\Gamma}$ with $\Gamma = 1.5$, since local sources have $\Gamma \geq 2$.

Three approaches to calculate the EBL:

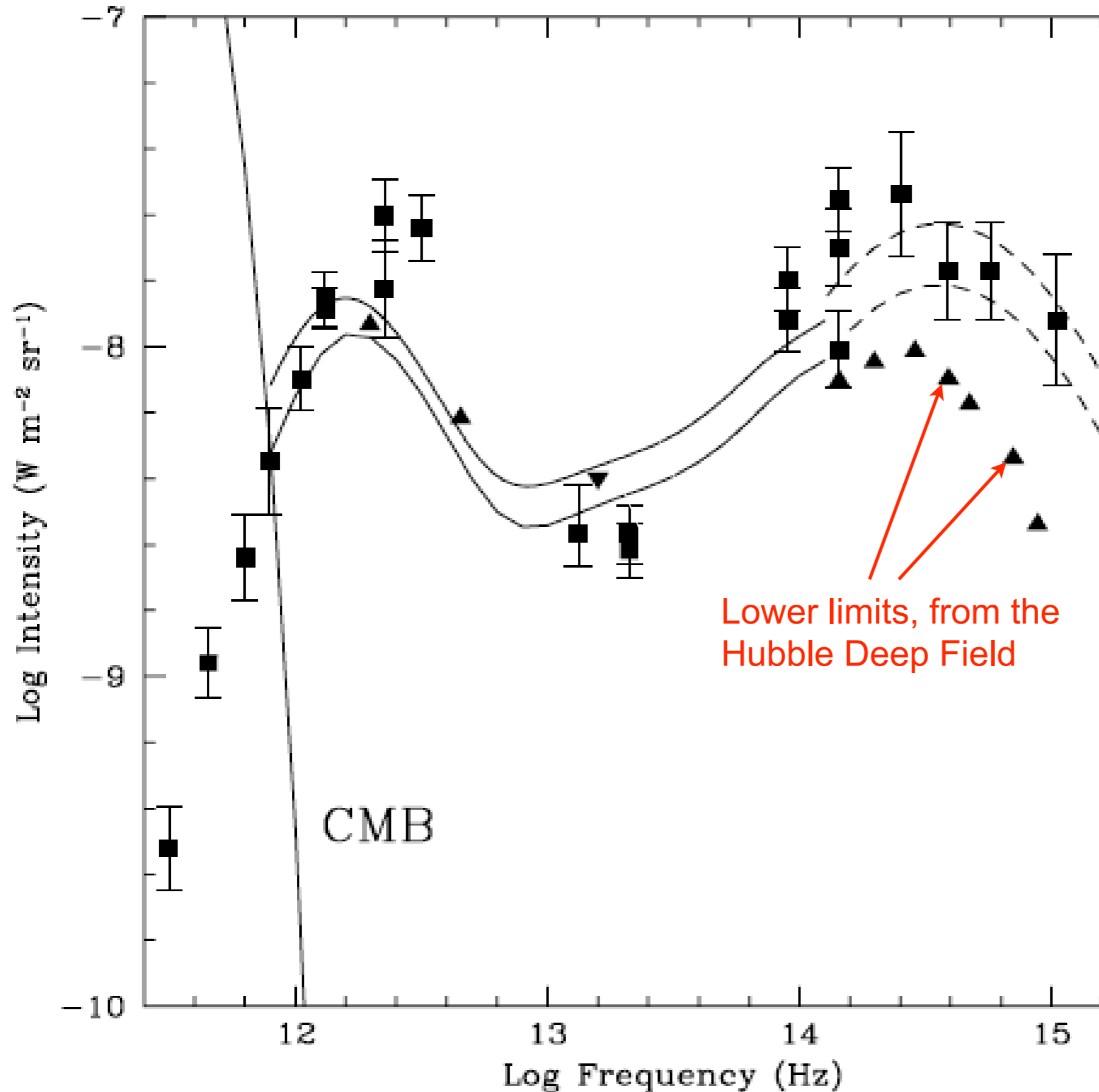
Backward Evolution, which starts with the existing galaxy population and evolves it backward in time -- e.g., Stecker, Malkan, & Scully 2006. Dangerous!

Evolution Inferred from Observations -- e.g., Kneiske et al. 2002; Franceschini et al. 2008; Dominguez, Primack, et al. in prep. using AEGIS data.

Forward Evolution, which begins with cosmological initial conditions and models gas cooling, **formation of galaxies including stars and AGN**, feedback from these phenomena, and light absorption and re-emission by **dust**.

All methods currently require modeling galactic SEDs. **Forward Evolution** requires semi-analytic models (SAMs) based on cosmological simulations.

Backward Evolution



A problem with this approach is that high- z galaxies are very different from low- z galaxies.

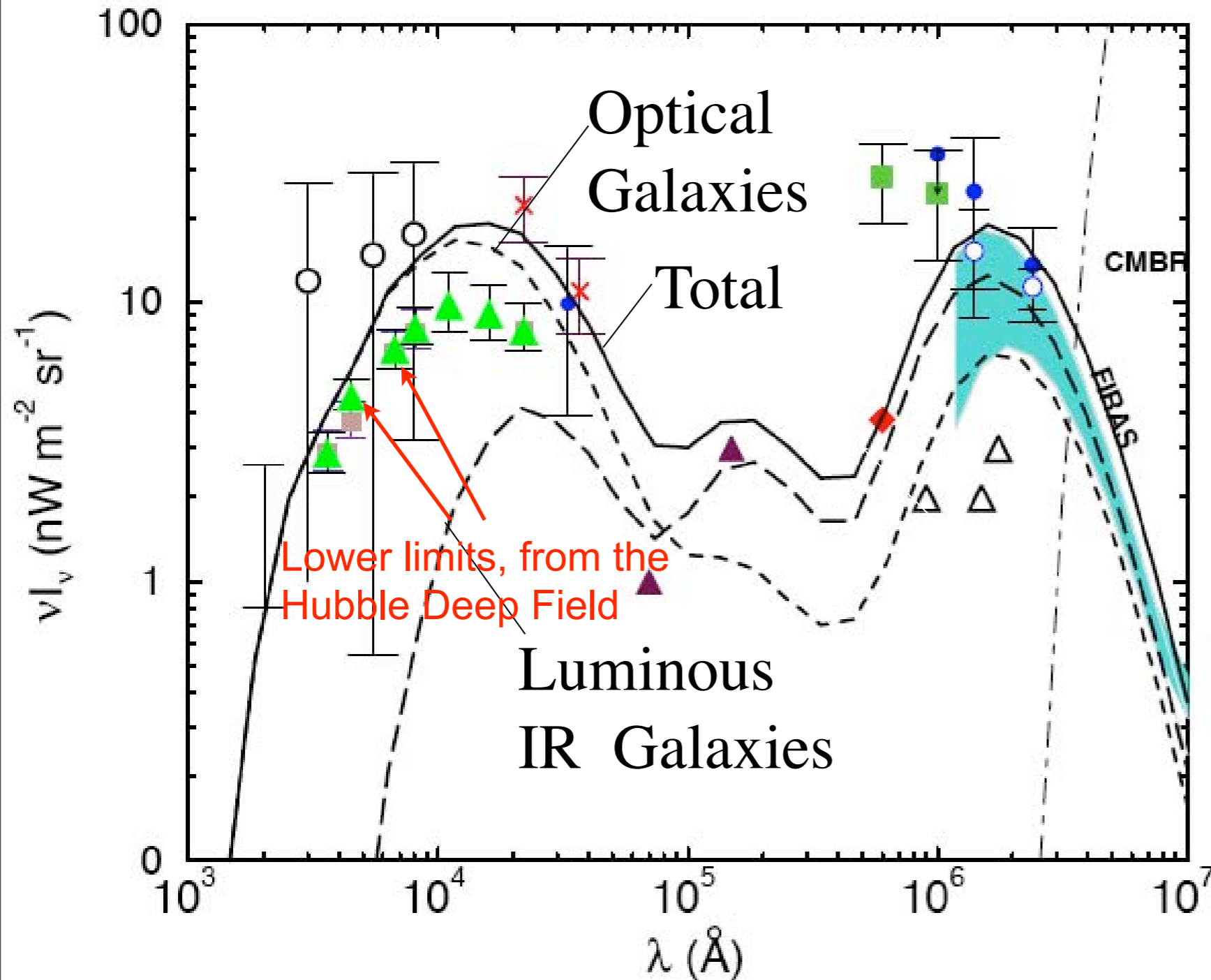
F. W. Stecker,
M. A. Malkan,
& S. T. Scully 2006

Fast Evolution:
galaxy luminosities evolve
as $(1+z)^4$ for $0 < z < 0.8$,
as $(1+z)^2$ for $0.8 < z < 1.5$,
no evolution $1.5 < z < 6$,
zero luminosity for $z > 6$.

Baseline Model:
galaxy luminosities evolve
as $(1+z)^{3.1}$ for $0 < z < 1.4$,
no evolution $1.4 < z < 6$,
zero luminosity for $z > 6$.

Evolution Inferred from Observations

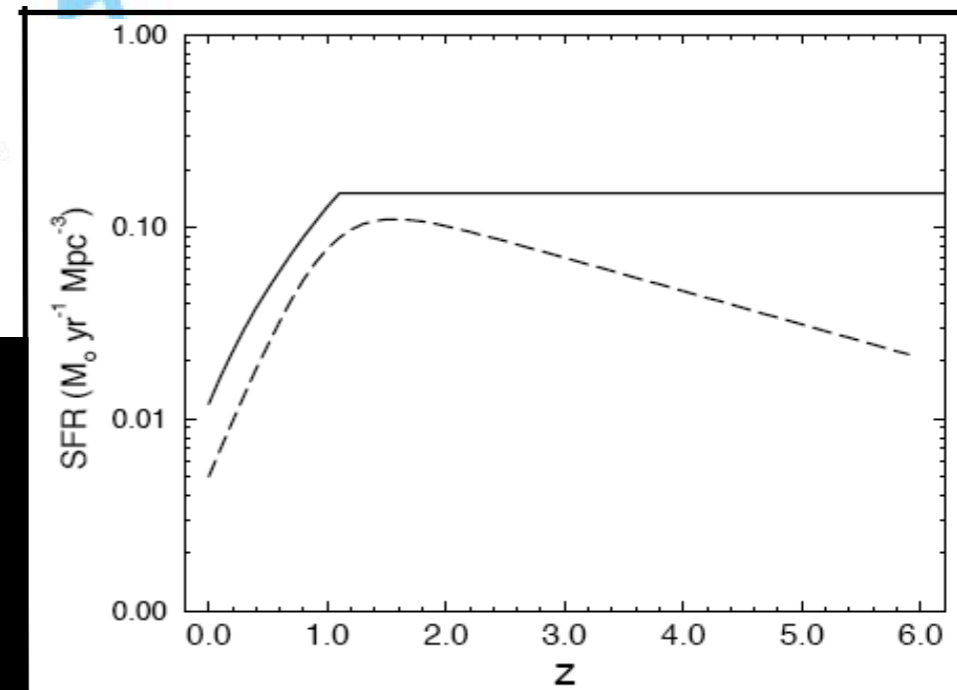
T. M. Kneiske et al.: Implications of cosmological gamma-ray absorption. I. 2002



- ▲ HST Pozetti et al. 1998,2000
- Bernstein et al. 2001
- × Gorjan et al. 2000
- ▲ ISOCAM Altieri et al. 1999
- ◆ IRAS Hacking & Soifer 1991
- Finkbeiner et al. 2000
- △ Juvella et al 2000
- DIRBE Dwek & Arendt 1998 (NIR)
Hauser et al 1998 (FIR)
- corrected with WIM Lagache et al 1999
- ▭ FIRAS Fixsen et al. 1997

Lower limits, from the Hubble Deep Field

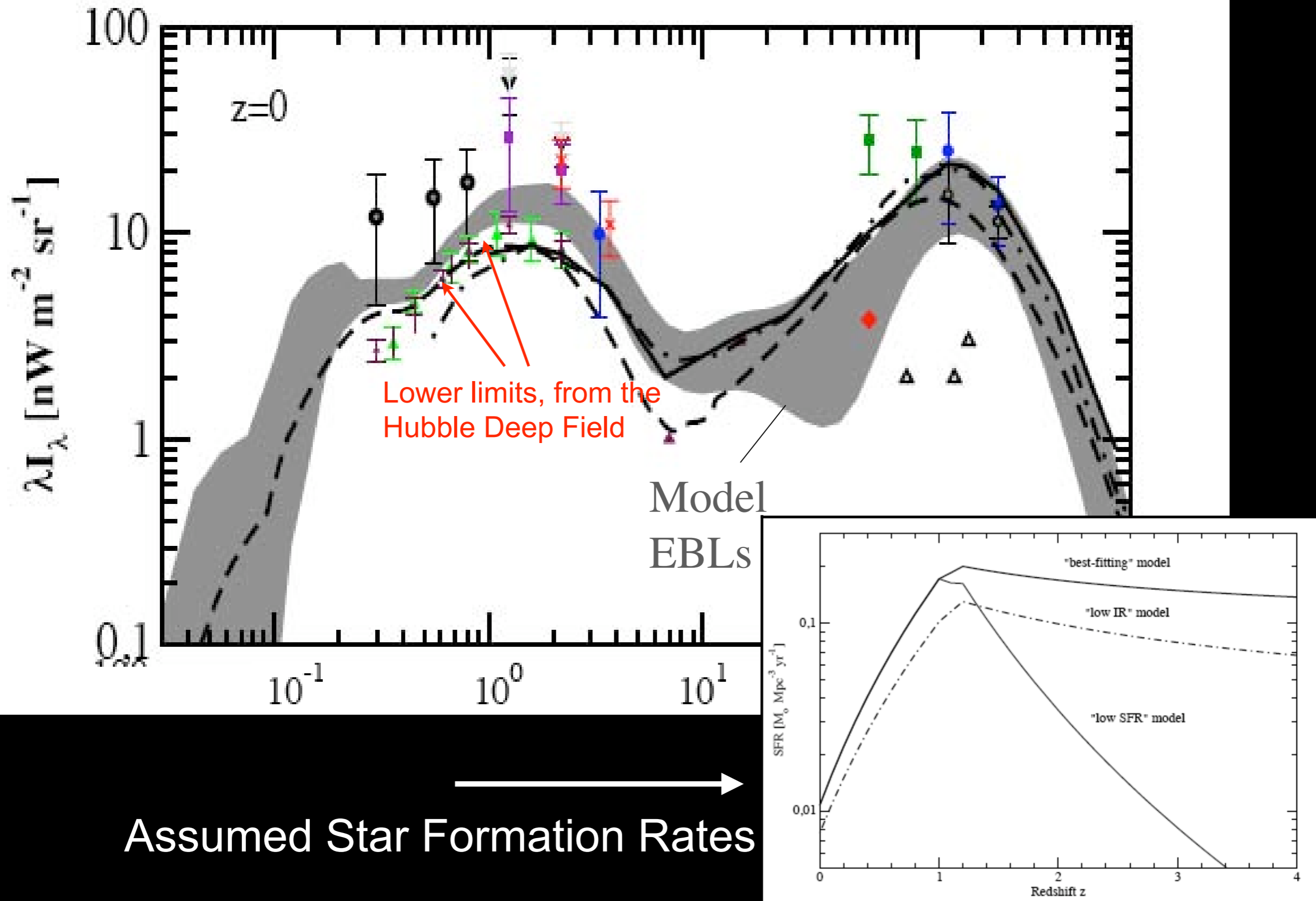
Assumed Star Formation Rate
(solid curve)



Evolution Inferred from Observations

T. M. Kneiske et al.: Implications of cosmological gamma-ray absorption. II.

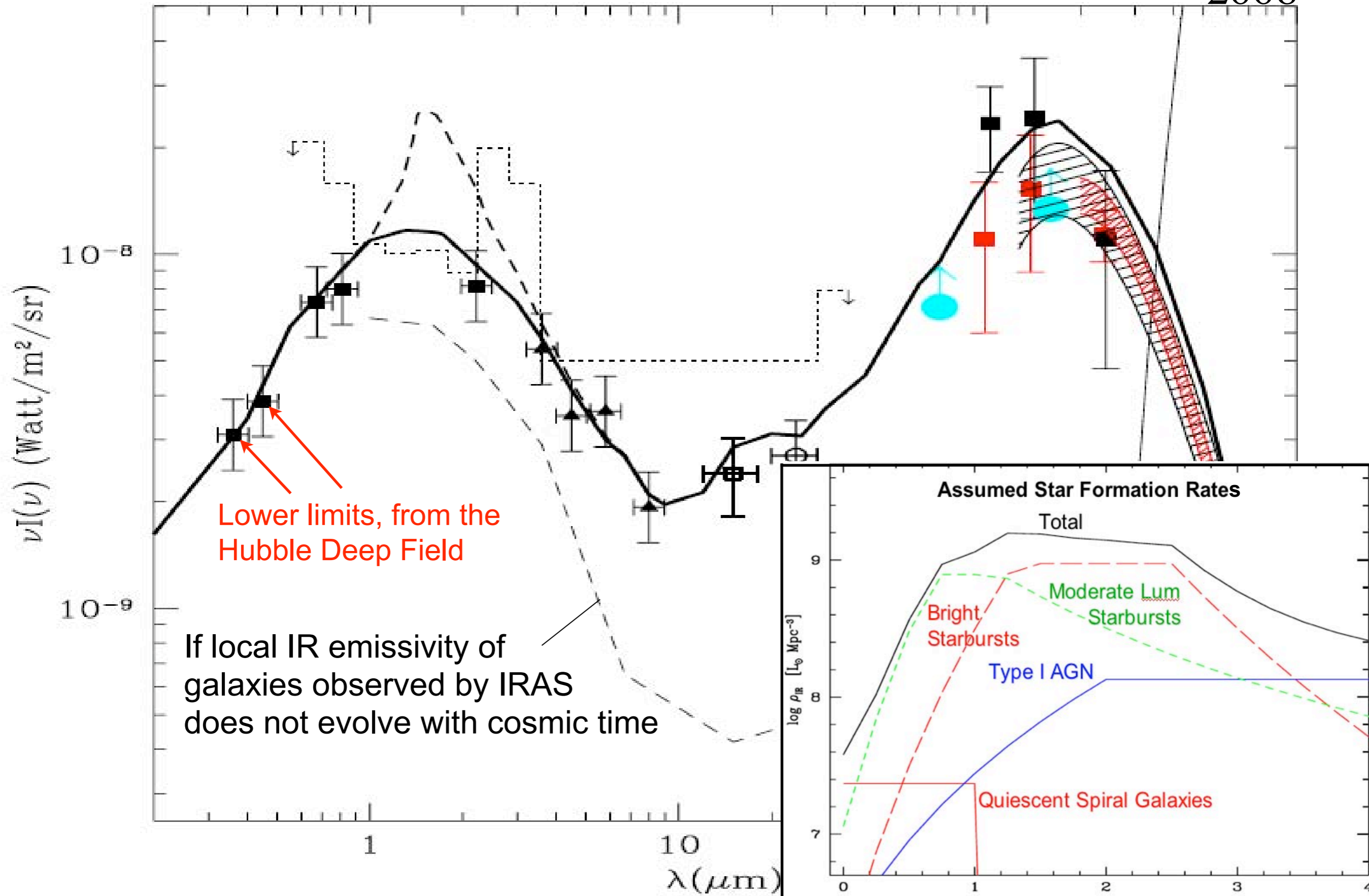
2004



Evolution Inferred from Observations

A. Franceschini, G. Rodighiero, M. Vaccari: Background radiations and the cosmic photon-photon opacity

2008

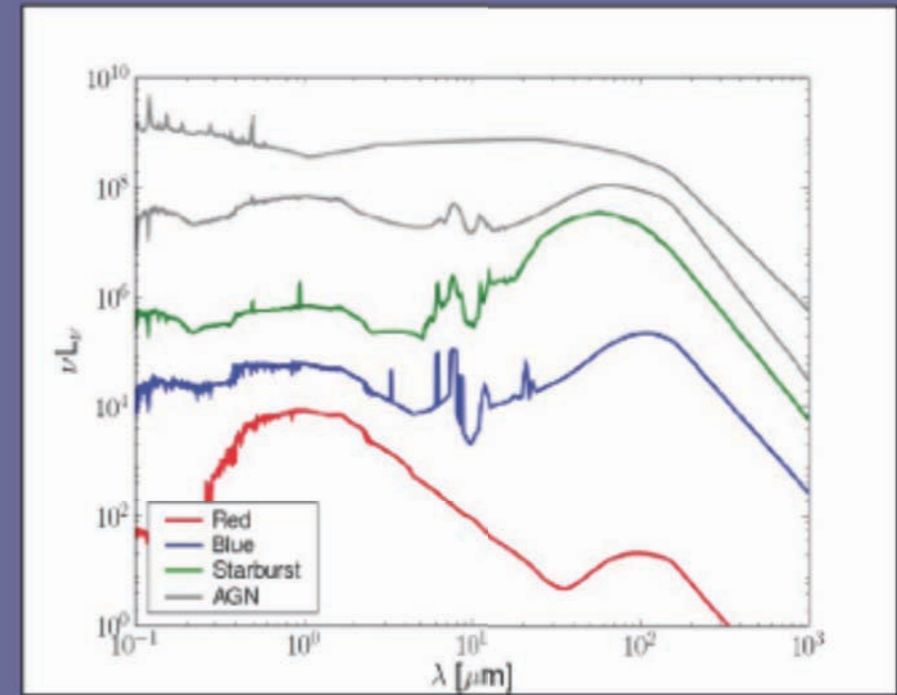


Evolution Inferred from Observations Using AEGIS Multiwavelength Data

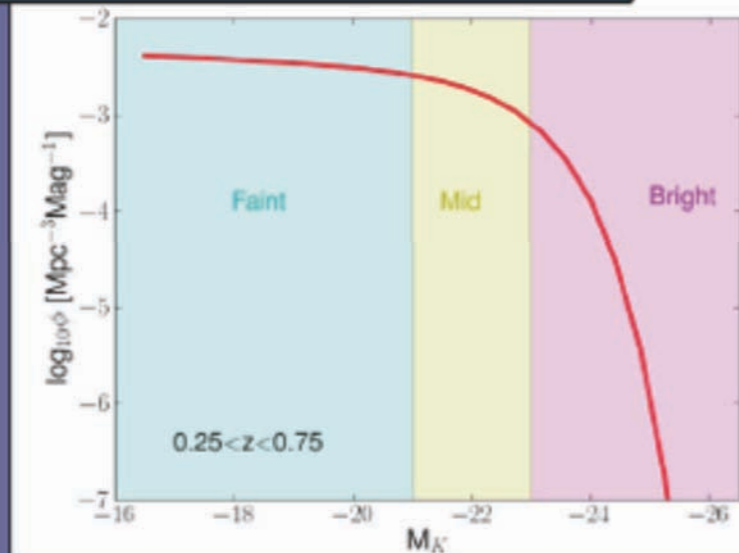
Alberto Dominguez et al. (in prep.)

$$\begin{aligned}
 j_i(\lambda, z) &= j_i^{faint} + j_i^{mid} + j_i^{bright} = \\
 &= \int_{M_1}^{M_2} \underbrace{\Phi(M_K, z)}_{\text{grey}} \underbrace{f_i}_{\text{blue}} \underbrace{T_i(M_K, \lambda)}_{\text{red}} dM_K + \\
 &+ \int_{M_2}^{M_3} \underbrace{\Phi(M_K, z)}_{\text{grey}} \underbrace{m_i}_{\text{blue}} \underbrace{T_i(M_K, \lambda)}_{\text{red}} dM_K + \\
 &+ \int_{M_3}^{M_4} \underbrace{\Phi(M_K, z)}_{\text{grey}} \underbrace{b_i}_{\text{blue}} \underbrace{T_i(M_K, \lambda)}_{\text{red}} dM_K
 \end{aligned}$$

Spectral energy distributions
SWIRE template library, Polletta+ 07



Luminosity function
observed K-band, Cirasuolo+ 09

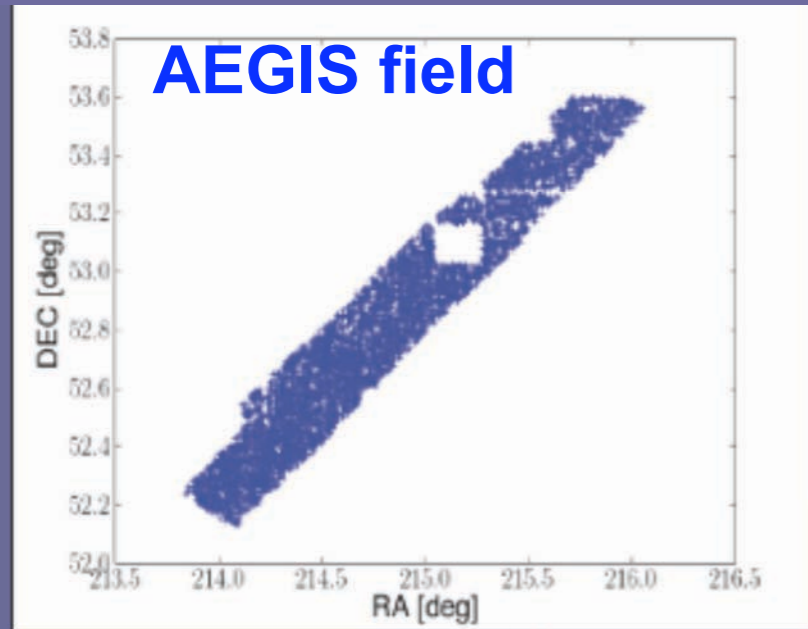


Spectral-type fractions

$$\lambda I_\lambda(z) = \frac{c}{4\pi} \int_z^{z_{max}} j_{total}[\lambda(1+z)/(1+z'), z'] \left| \frac{dt}{dz'} \right| dz'$$

Evolution Inferred from Observations Using AEGIS Multiwavelength Data

Alberto Dominguez et al. (in prep.)



total sample 5986 objects

AEGIS multi-wavelength sample

Detection:

B, R, I, Ks, IRAC 3.6

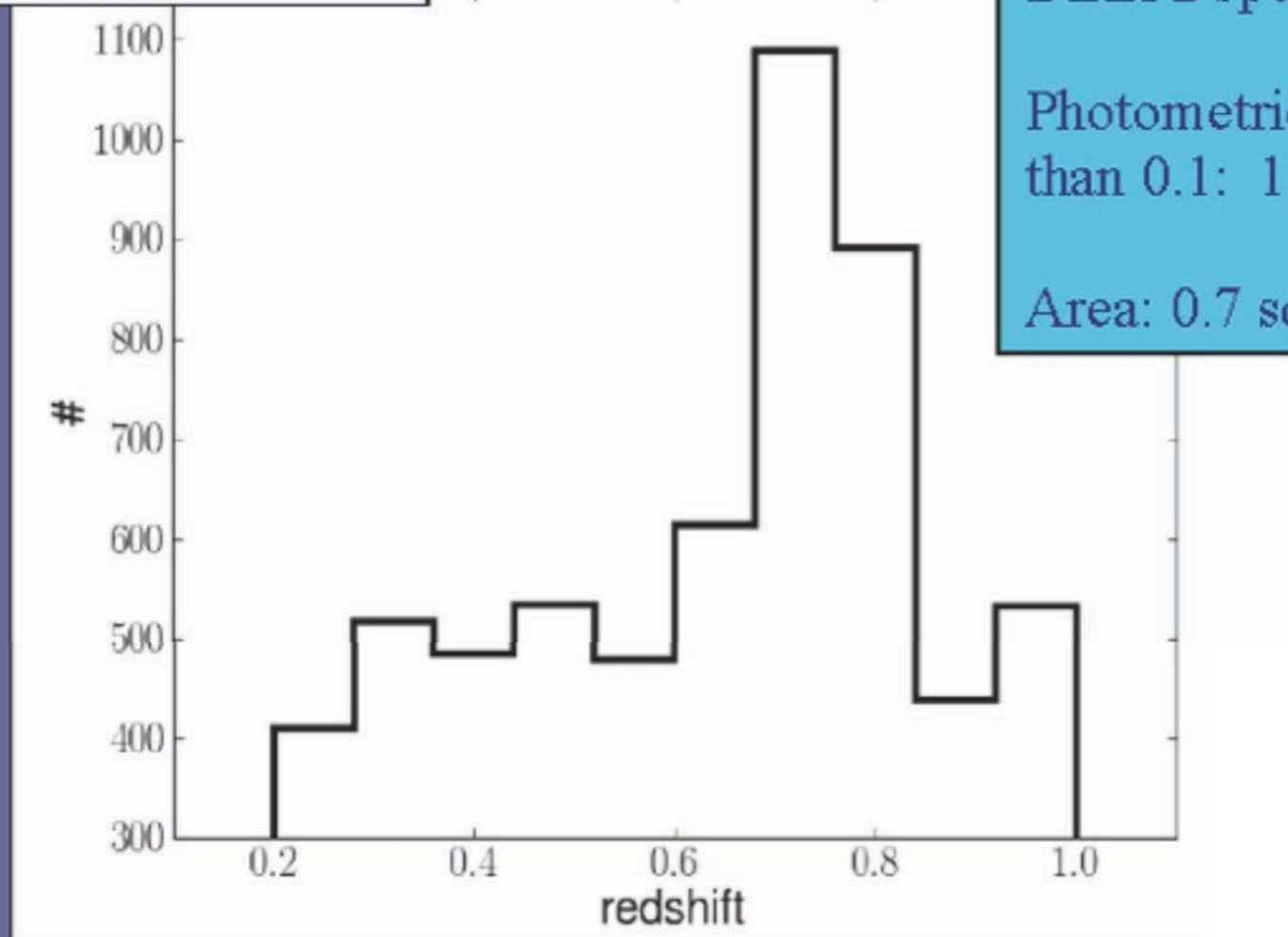
Observation:

IRAC 4.5, IRAC 5.8, IRAC 8, MIPS 24

DEEP2 spectroscopic redshift: 4376 galaxies

Photometric redshift with mean error less than 0.1: 1610 galaxies

Area: 0.7 sq deg



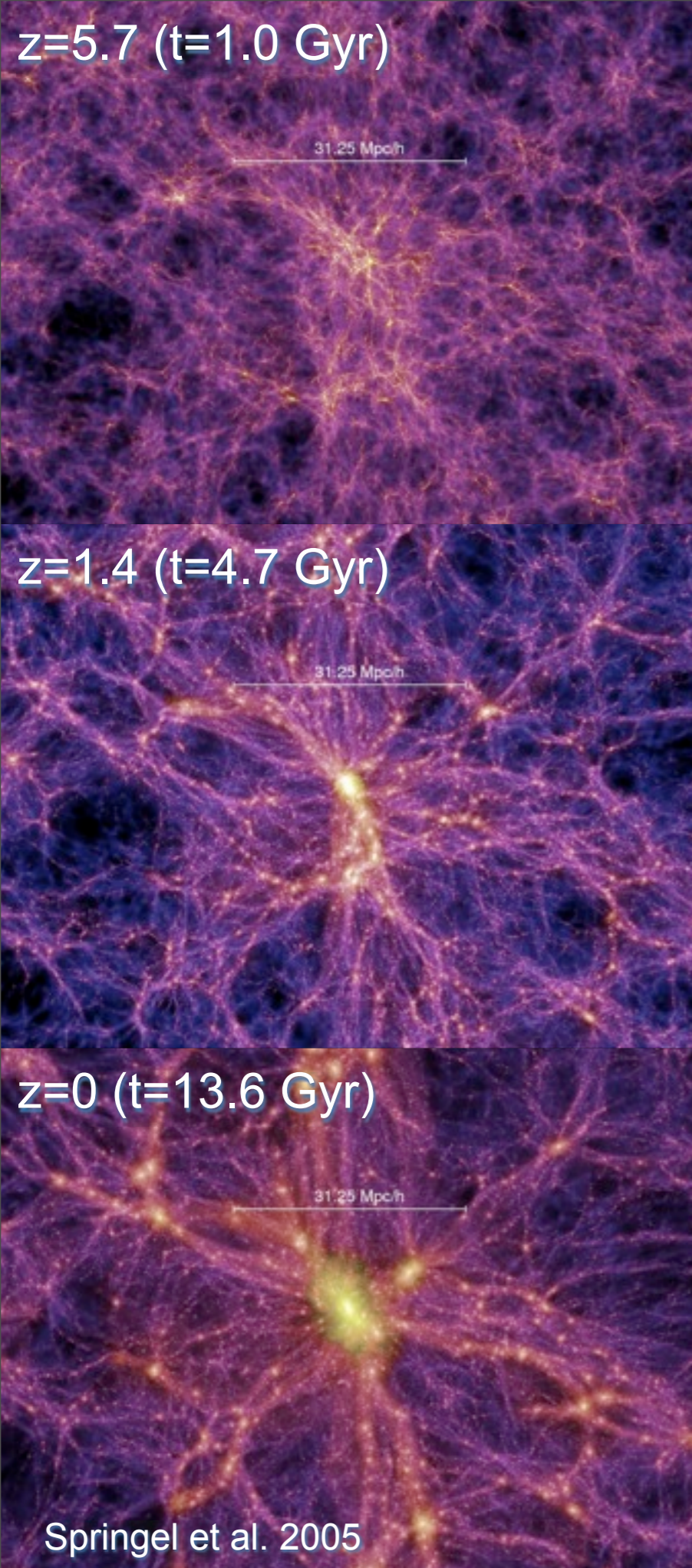
High redshift $z > 1$

Either assume SED types are constant, or else make extreme assumptions to bound the uncertainty.

Forward Evolution

When we first tried doing this (Primack & MacMinn 1996), both the stellar initial mass function (IMF) and the values of the cosmological parameters were quite uncertain. After 1998, the cosmological model was known to be Λ CDM although it was still necessary to consider various cosmological parameters in models. Now the parameters are known rather precisely, and my report here is based on a semi-analytic model (SAM) using the current (WMAP5) cosmological parameters. With improved simulations and better galaxy data, we can now normalize SAMs better and determine the key astrophysical processes to include in them.

There is still uncertainty whether the IMF evolves, possibly becoming “top-heavy” at higher redshifts (Fardal et al. 2007, Dave 2008), and uncertainty concerning the nature of sub-mm galaxies and the feedback from AGN.



Forward Evolution



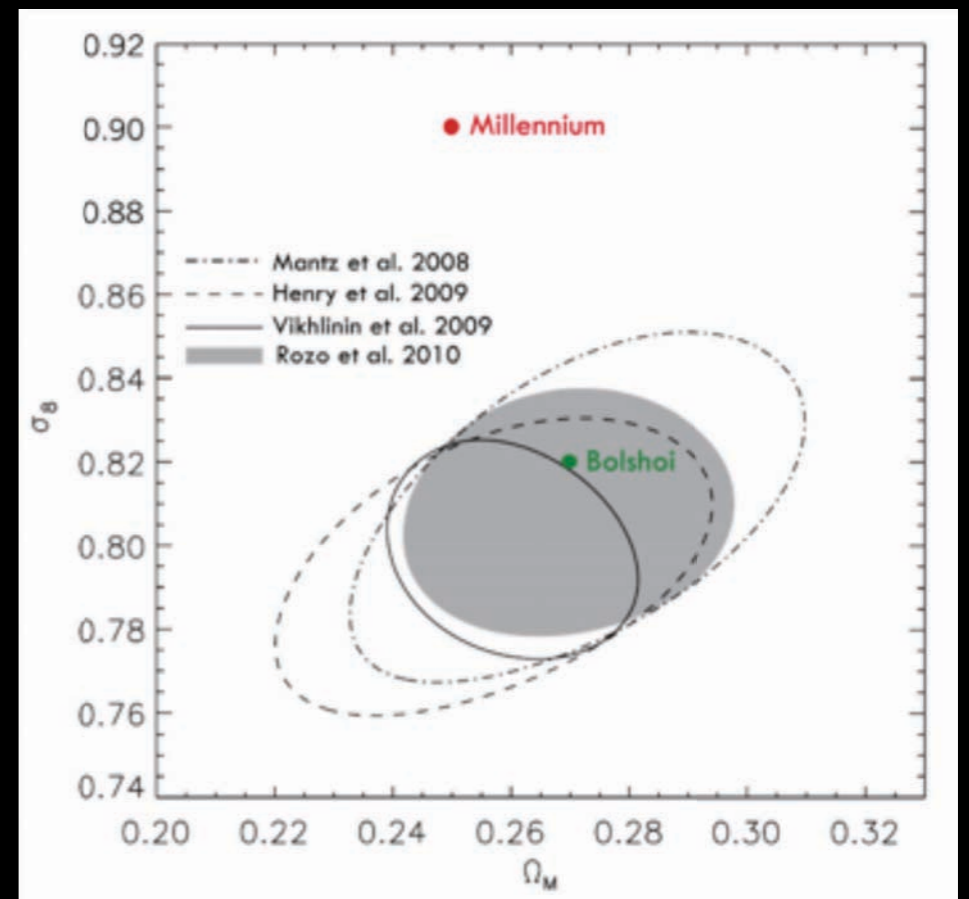
time



Wechsler et al. 2002

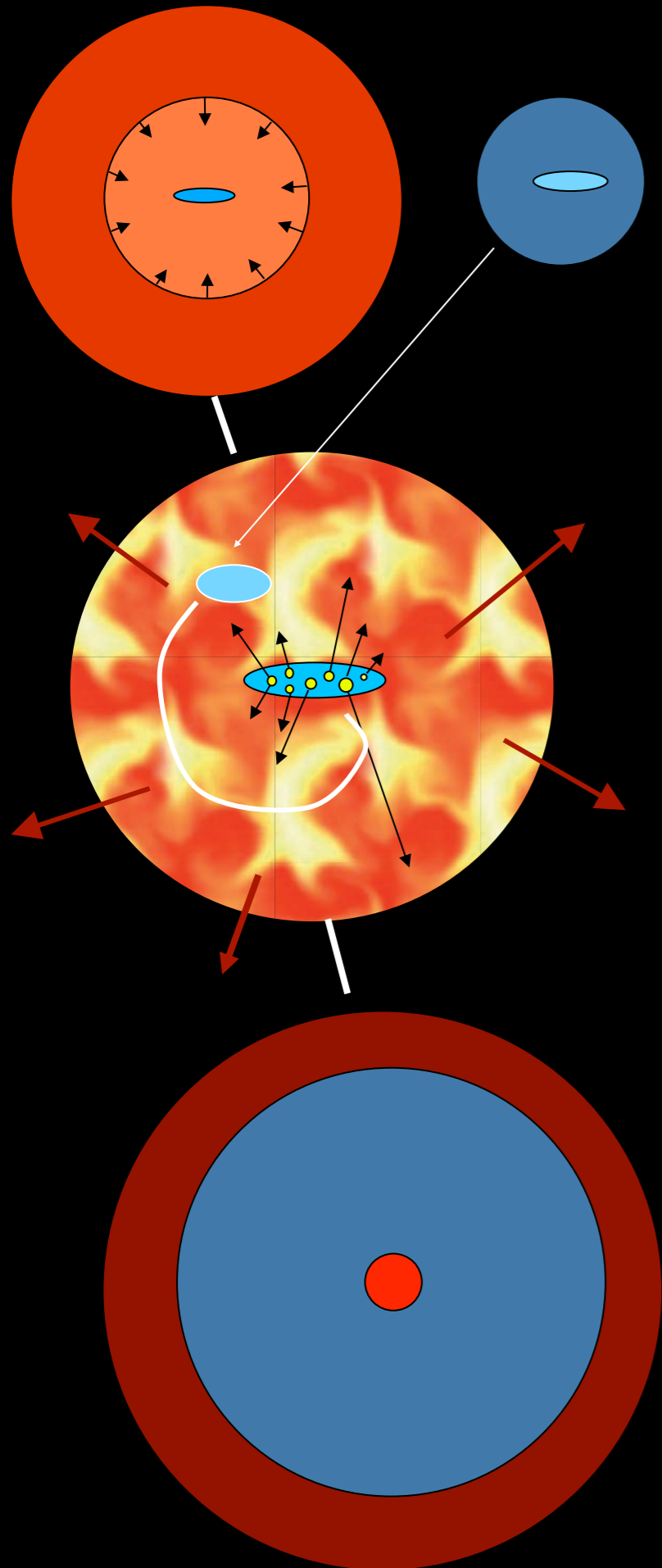
Present status of Λ CDM
 “Double Dark” theory:

- cosmological parameters are now well constrained by observations



- mass accretion history of dark matter halos is represented by ‘merger trees’ like the one at left

Galaxy Formation in Λ CDM

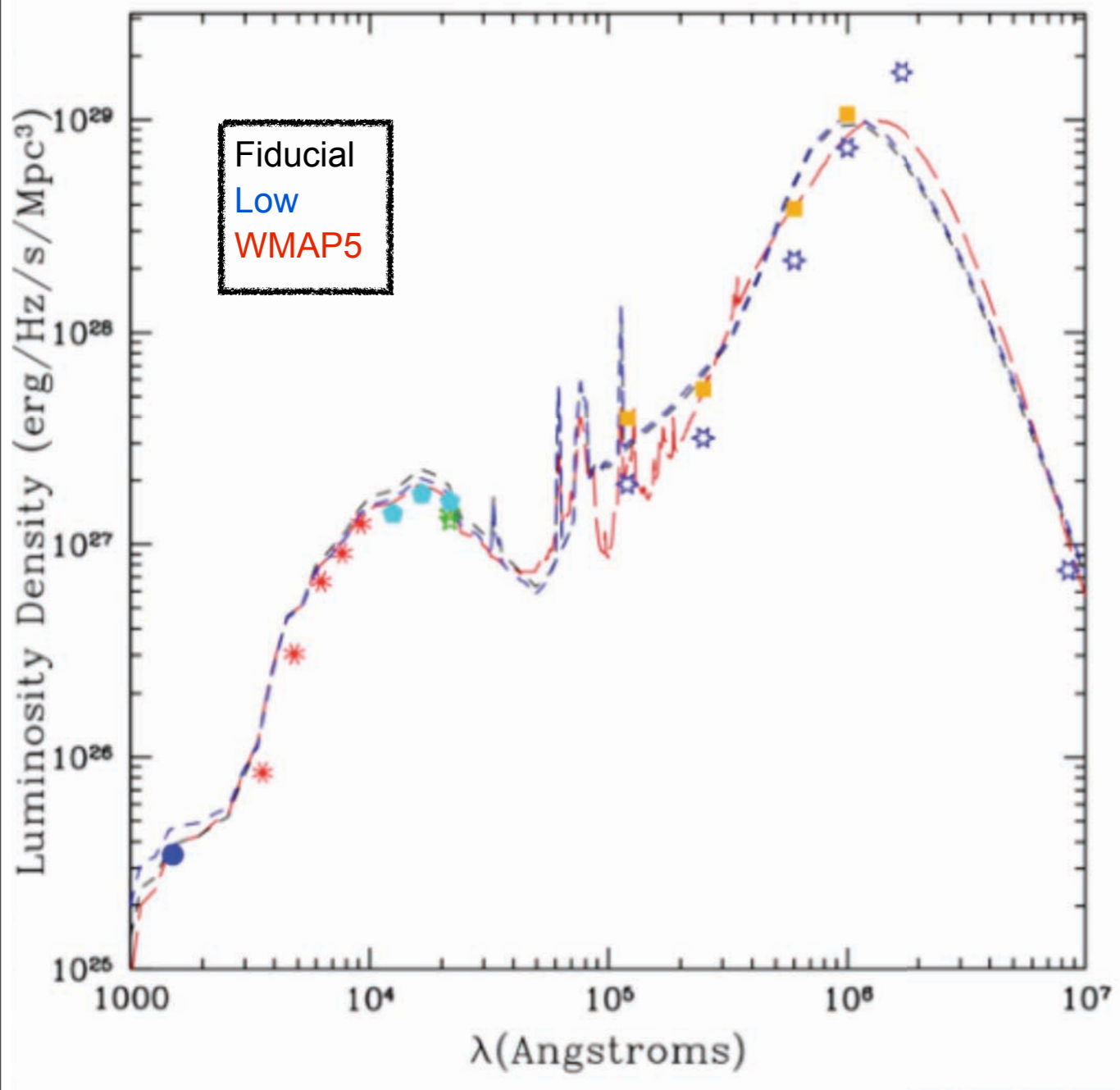


- gas is collisionally heated when perturbations ‘turn around’ and collapse to form gravitationally bound structures
- gas in halos cools via atomic line transitions (depends on density, temperature, and metallicity)
- cooled gas collapses to form a rotationally supported disk
- cold gas forms stars, with efficiency a function of gas density (e.g. Schmidt-Kennicutt Law)
- massive stars and SNa_e reheat (and in small halos expel) cold gas and some metals
- galaxy mergers trigger bursts of star formation; ‘major’ mergers transform disks into spheroids and fuel AGN
- AGN feedback cuts off star formation

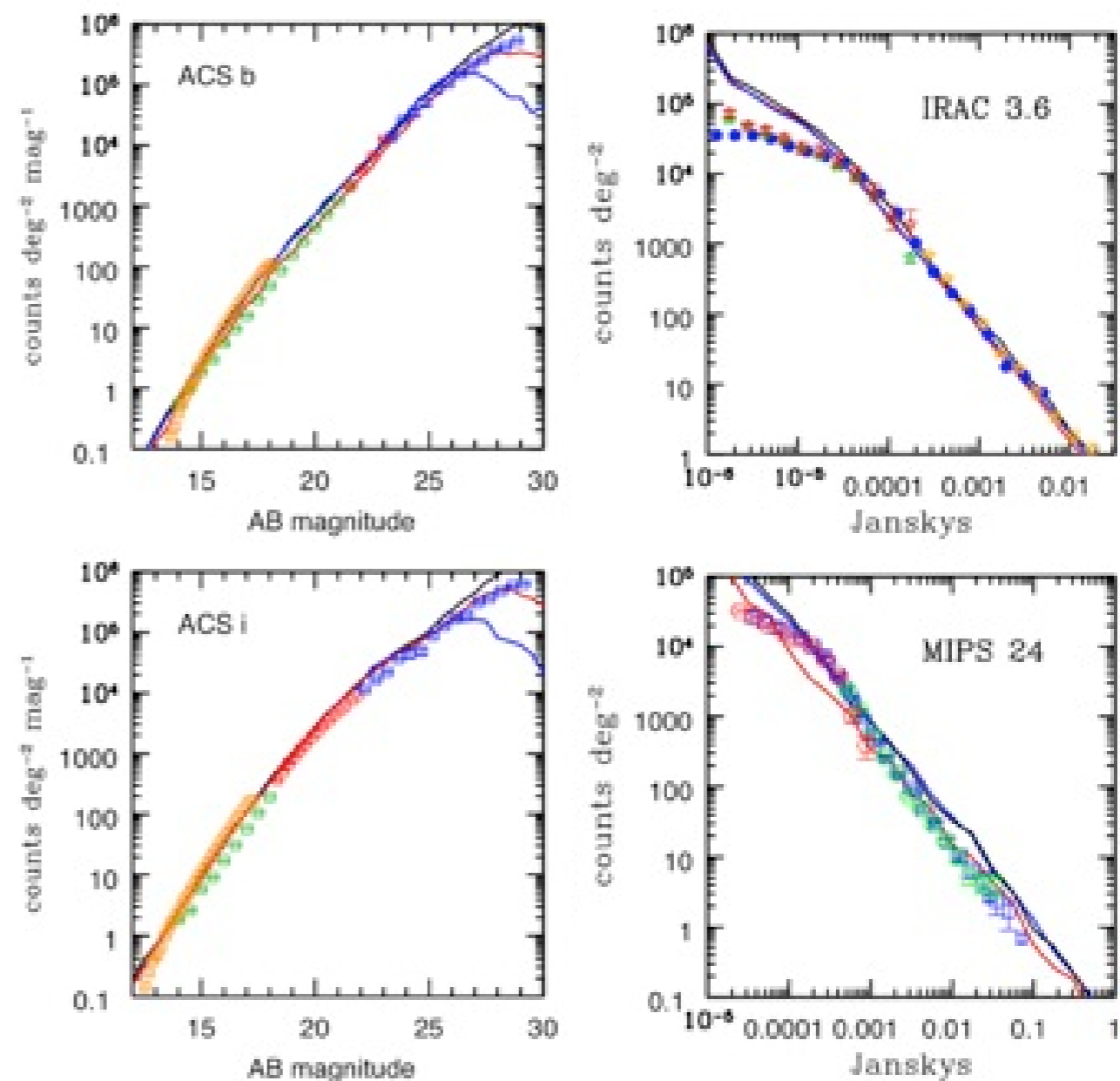
White & Frenk 1991; Kauffmann et al. 1993; Cole et al. 1994; Somerville & Primack 1999; Cole et al. 2000; Somerville, Primack, & Faber 2001; Croton et al. 2006; Somerville et al. 2008; Fanidakis et al. 2009; Somerville, Gilmore, & Primack, in prep.

Some Results from our Semi-Analytic Models

$z=0$ Luminosity Density

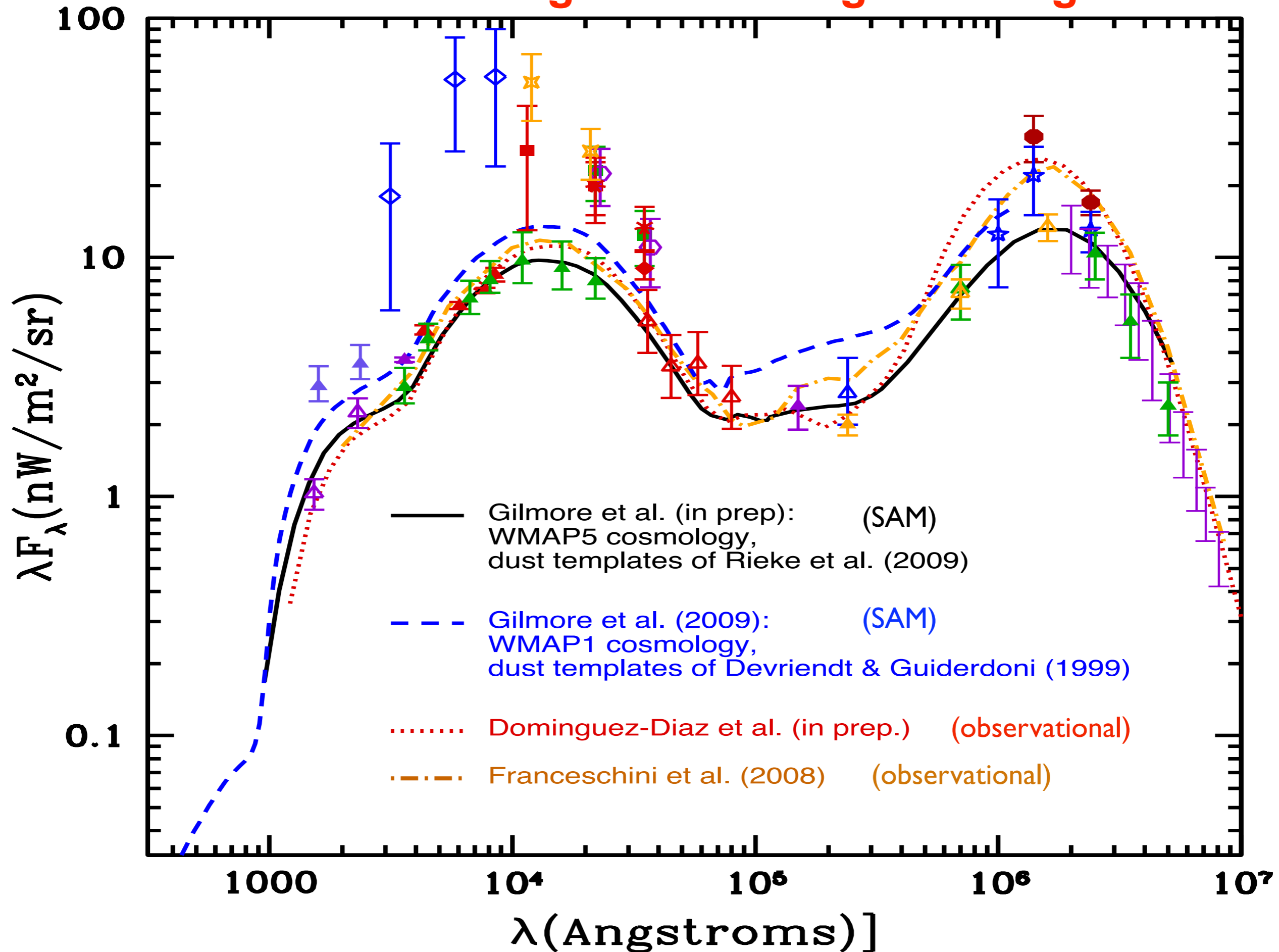


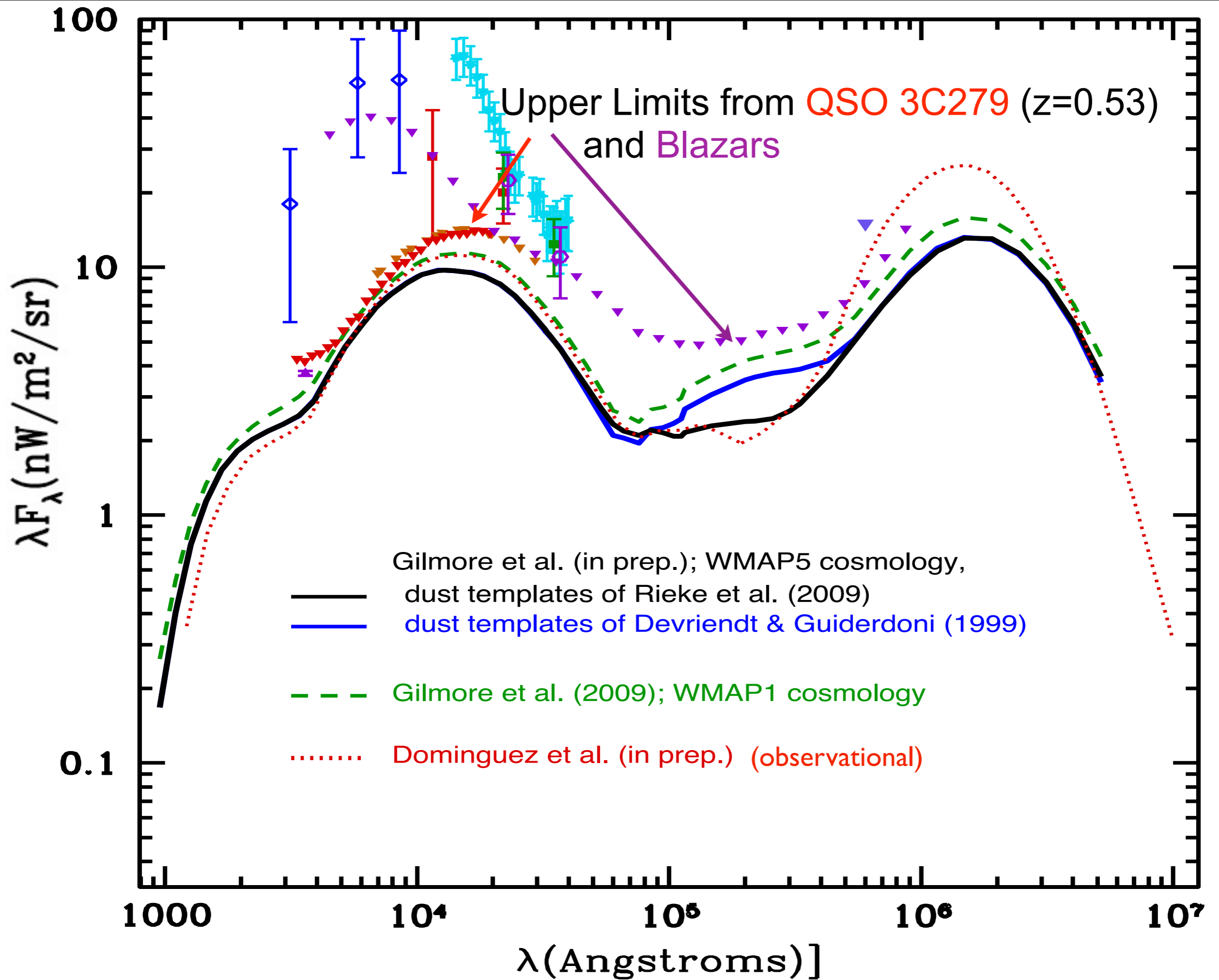
Number Counts in b, i, 3.6 and 24 μm Bands



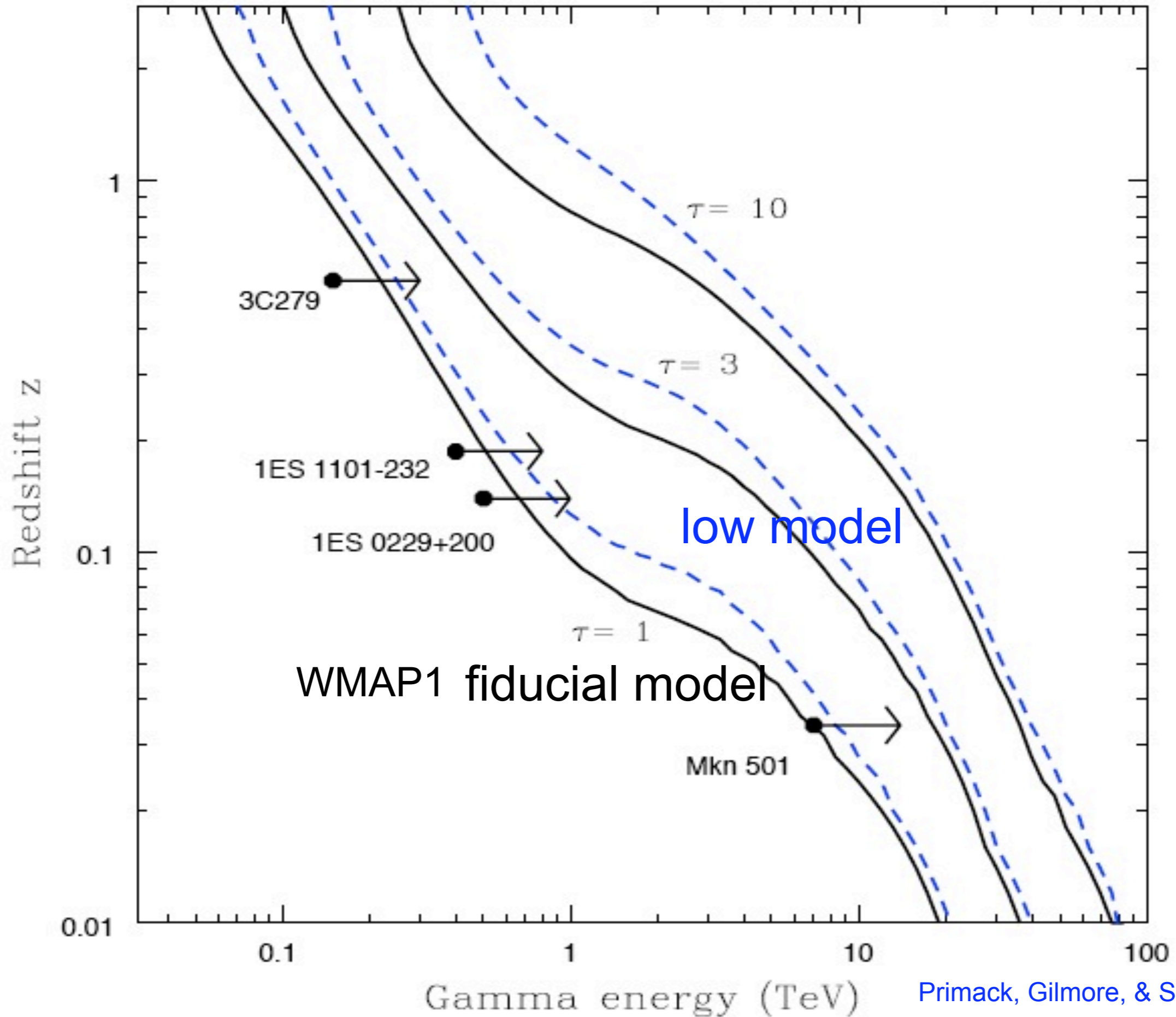
Somerville, Gilmore, & Primack (in prep.)

Local Extragalactic Background Light



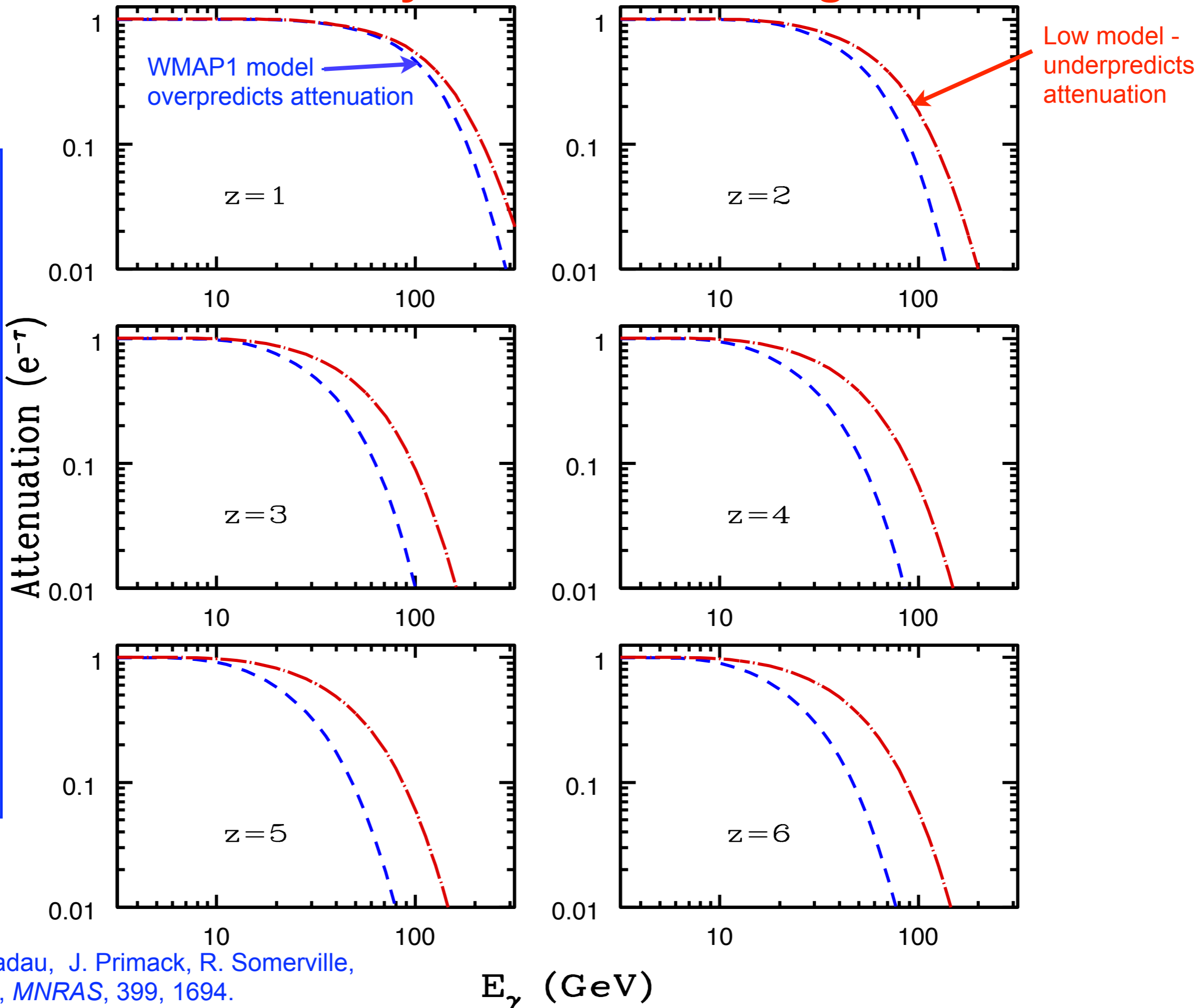


Gamma Ray Attenuation Predictions vs. Observational Limits



Predicted Gamma Ray Attenuation at High Redshifts

Our models are based on varying the SFR, ionizing light escape fraction from galaxies, and UV from AGN. Our models include radiative transfer through the IGM.



R. Gilmore, P. Madau, J. Primack, R. Somerville,
& F. Haardt 2009, *MNRAS*, 399, 1694.

Modelling gamma-ray burst observations by *Fermi* and MAGIC including attenuation due to diffuse background light

Rudy C. Gilmore,^{1★} Francisco Prada^{2†} and Joel Primack¹

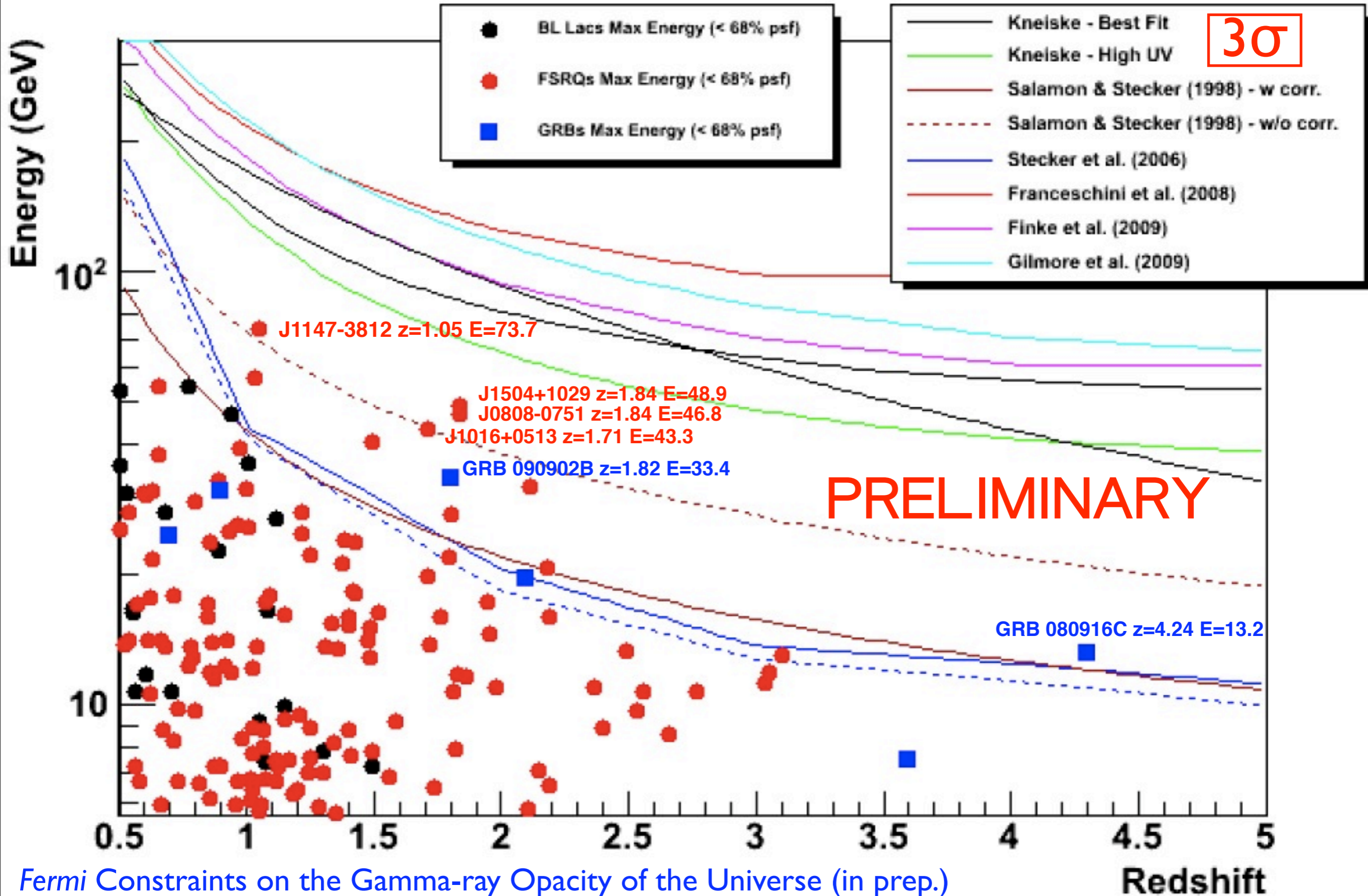
¹*Department of Physics, University of California, Santa Cruz, CA 95064, USA*

²*Instituto de Astrofísica de Andalucía, CSIC, Apdo. Correos 3004, E-18080 Granada, Spain*

ABSTRACT

Gamma rays from extragalactic sources are attenuated by pair-production interactions with diffuse photons of the extragalactic background light (EBL). Gamma-ray bursts (GRBs) are a source of high-redshift photons above 10 GeV, and could be therefore useful as a probe of the evolving ultraviolet background radiation. In this paper, we develop a simple phenomenological model for the number and redshift distribution of GRBs that can be seen at GeV energies with the *Fermi* satellite and Major Atmospheric Gamma-ray Imaging Cherenkov Telescope (MAGIC) atmospheric Cherenkov telescope. We estimate the observed number of gamma rays per year, and show how this result is modified by considering interactions with different realizations of the evolving EBL. We also discuss the bright *Fermi* GRB 080916C in the context of this model. We find that the Large Area Telescope on *Fermi* can be expected to see a small number of photons above 10 GeV each year from distant GRBs. Annual results for ground-based instruments like MAGIC are highly variable due to the low duty cycle and sky coverage of the telescope. However, successfully viewing a bright or intermediate GRB from the ground could provide hundreds of photons from high redshift, which would almost certainly be extremely useful in constraining both GRB physics and the high-redshift EBL.

Fermi highest-energy photons from blazars and GRBs vs. redshift



PRELIMINARY

Fermi Constraints on the Gamma-ray Opacity of the Universe (in prep.)

from the draft
Conclusions

Using high-energy 11-month photon data set collected by Fermi from distant blazars and GRBs we have (i) **constrained the opacity of the universe to rays in the $\sim 10\text{--}100$ GeV range and coming from various redshifts up to $z \approx 4.35$** ; and (ii) **ruled out an EBL intensity as high as predicted by Stecker et al. (2006) in the optical–ultraviolet range at more than 4σ in five independent sources, thereby resulting in a $> 5\sigma$ rejection significance level in total.** Our most constraining results come from blazars J1504+1029, J0808-0751 and J1016+0513 with (z, E_{max}) combinations of (1.84, 48.9 GeV), (1.84, 46.8 GeV) and (1.71, 43.3 GeV), respectively. The two most constraining **GRBs** are GRB 090902B and GRB 080916C, both of which **rule out the Stecker et al. (2006) EBL models in the UV energy range at more than 3σ level.**

Halos and galaxies: results from the Bolshoi simulation.

Anatoly A. Klypin¹, Sebastian Trujillo-Gomez¹, and Joel Primack² ¹NMSU, ²UCSC

ABSTRACT

Lambda Cold Dark Matter (Λ CDM) is now the standard theory of structure formation in the Universe. We present the first results from the new Bolshoi dissipationless cosmological Λ CDM simulation that uses cosmological parameters favored by current observations, which imply one-third fewer $10^{12}h^{-1}M_{\odot}$ dark matter halos than the WMAP1 (2003) parameters used in the Millennium simulations. The Bolshoi simulation was done in a volume $250 h^{-1}$ Mpc on a side using 8 billion particles with mass and force resolution adequate to follow subhalos down to a completeness limit of $V_{\text{circ}} = 50 \text{ km s}^{-1}$ maximum circular velocity. Using merger trees derived from analysis of 180 stored time-steps we find the circular velocities of satellites before they fall into their host halos. Using excellent statistics of halos and subhalos (~ 10 million at every moment and ~ 50 million over the whole history) we present accurate approximations for statistics such as the halo mass function, the concentrations for distinct halos and subhalos, abundance of halos as function of their circular velocity, the abundance and the spatial distribution of subhalos. We find that at high redshifts the concentration falls to a minimum of about 3.8 and then rises slightly for higher values of halo mass, a new result. We present approximations for the velocity and mass functions of distinct halos as a function of redshift. We find that while the Sheth-Tormen approximation for the mass function of halos found by spherical overdensity is quite accurate at low redshifts, the ST formula over-predicts the abundance of halos by nearly an order of magnitude by $z = 10$. We find that the number of subhalos scales with the circular velocity of the host halo as $\sqrt{V_{\text{host}}}$, and that subhalos have nearly the same radial distribution as dark matter particles at radii 0.3-2 times the host halo virial radius. The subhalo velocity function $N(> V_{\text{sub}})$ behaves as V_{circ}^{-3} . Combining our and Via Lactea-II results, we find that inside the virial radius of halos with $V_{\text{circ}} = 200 \text{ km s}^{-1}$ the number of satellites is $N(> V_{\text{sub}}) = (V_{\text{sub}}/58 \text{ km s}^{-1})^{-3}$ for satellite velocities in the range $4 \text{ km s}^{-1} < V_{\text{sub}} < 150 \text{ km s}^{-1}$. Finally, we use an abundance-matching procedure to assign r -band luminosities to dark matter halos as a function of halo V_{circ} , and find that the luminosity-velocity relation is in remarkably good agreement with the observed Tully-Fisher relation for V_{circ} in the range 50-200 km s^{-1} .

arXiv:1002.3660v2

250 Mpc/h Bolshoi

The Bolshoi simulation

ART code

250Mpc/h Box

ΛCDM

$s_8 = 0.83$

$h = 0.73$

8G particles

1kpc/h force resolution

$1e8 M_{\text{sun}}/h$ mass res

dynamical range 262,000

time-steps = 400,000

NASA AMES

supercomputing center

Pleiades computer

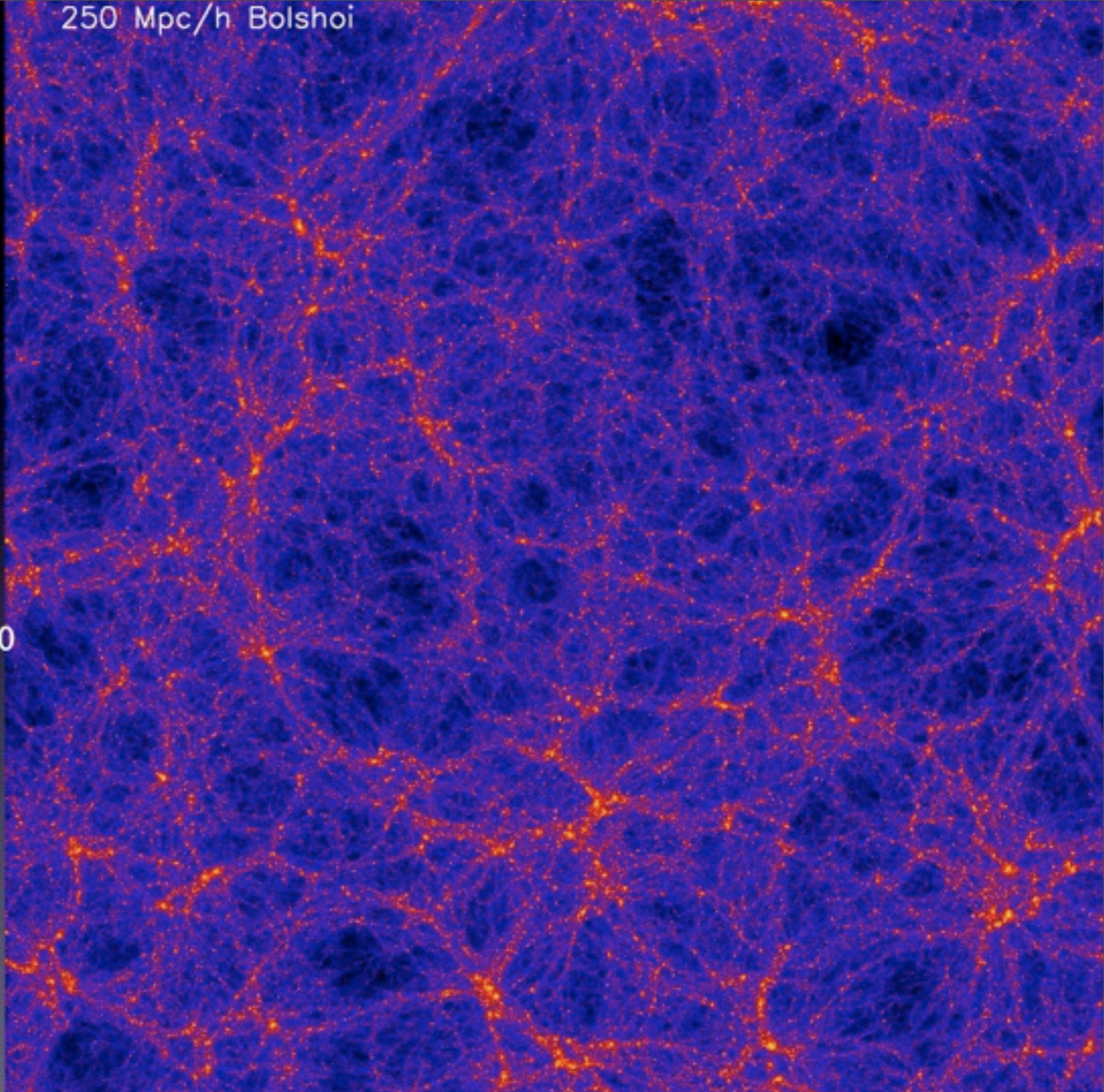
13824 cores

12TB RAM

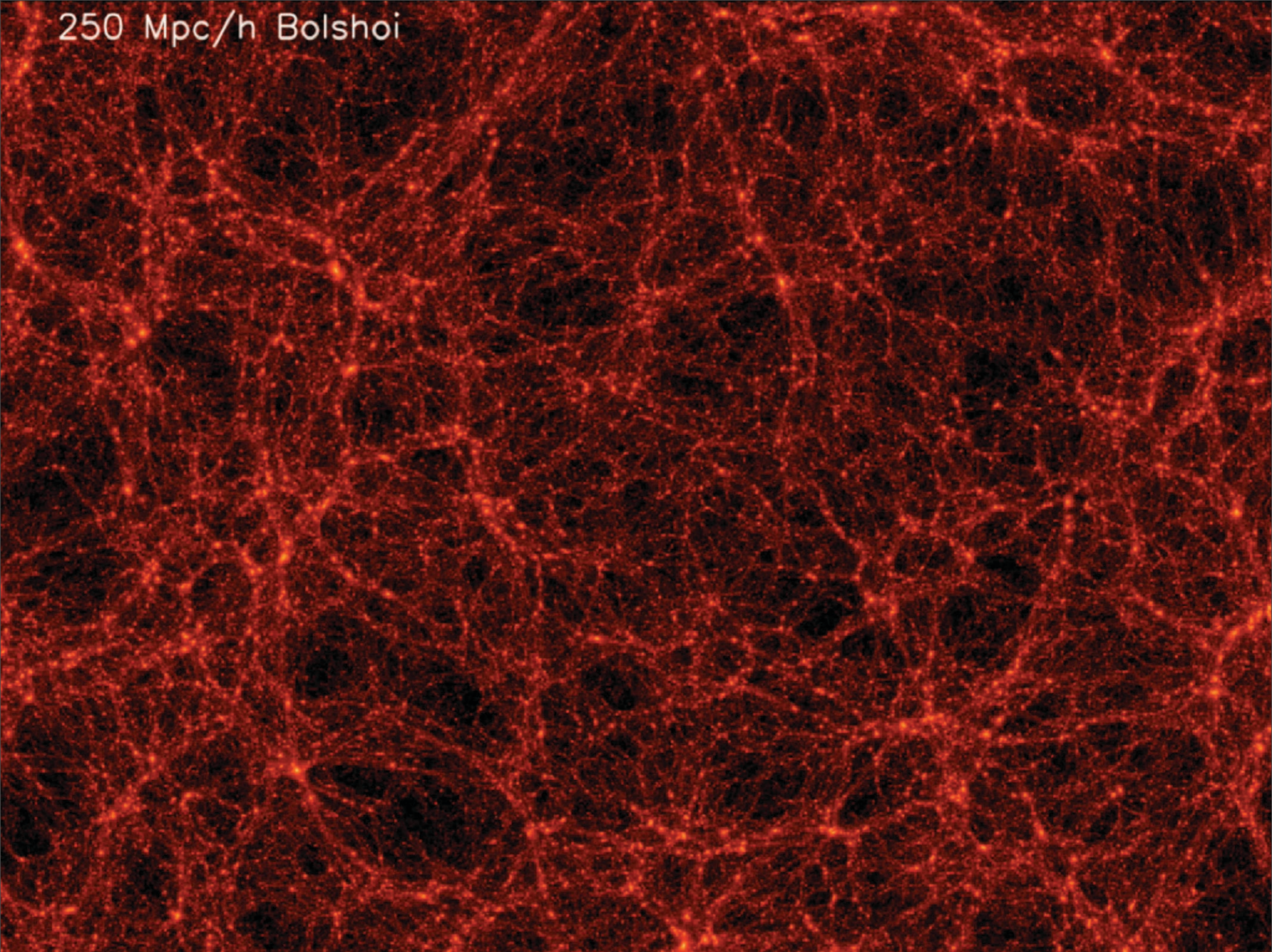
75TB disk storage

6M cpu hrs

18 days wall-clock time

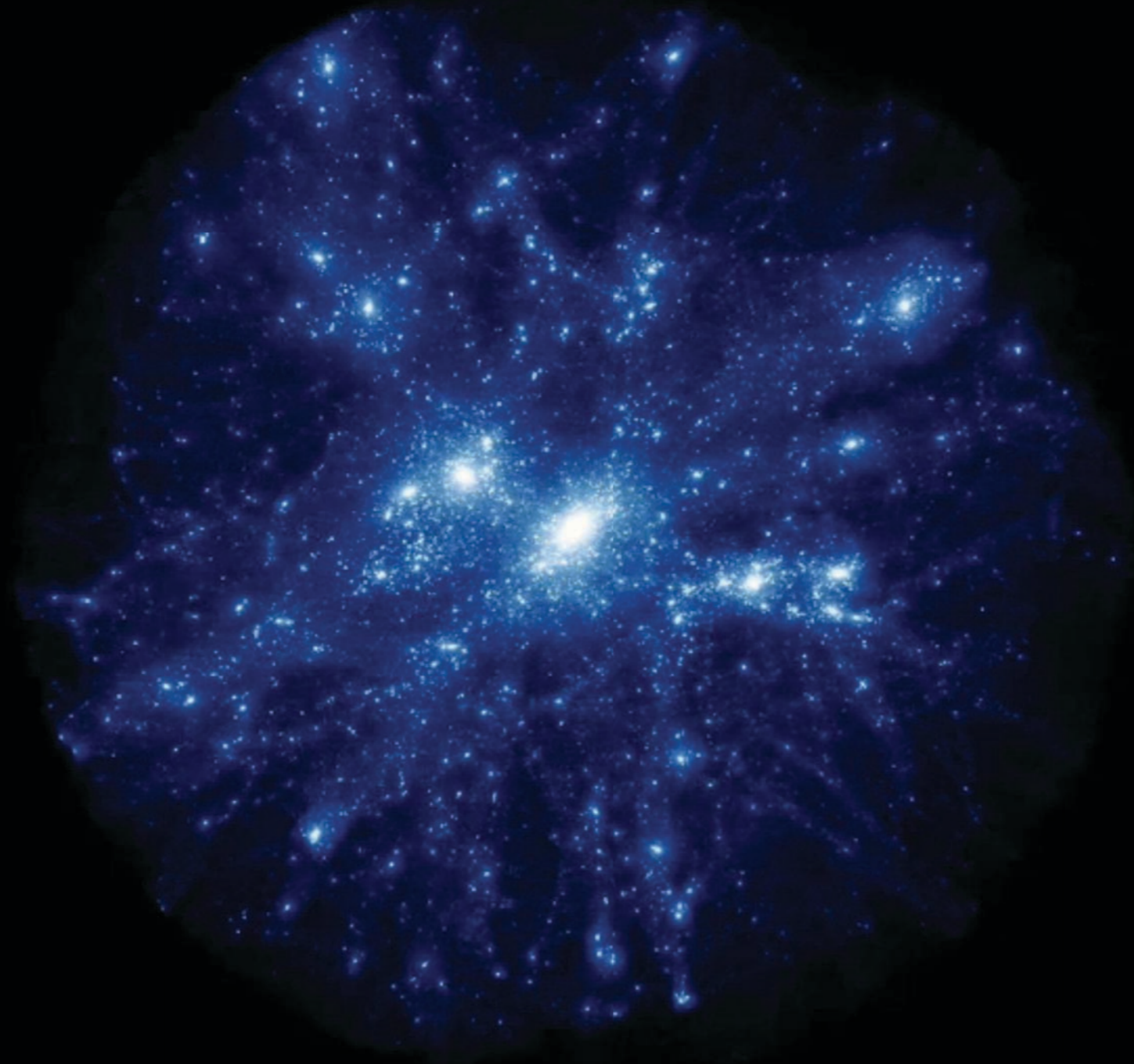


250 Mpc/h Bolshoi



Thursday, March 25, 2010

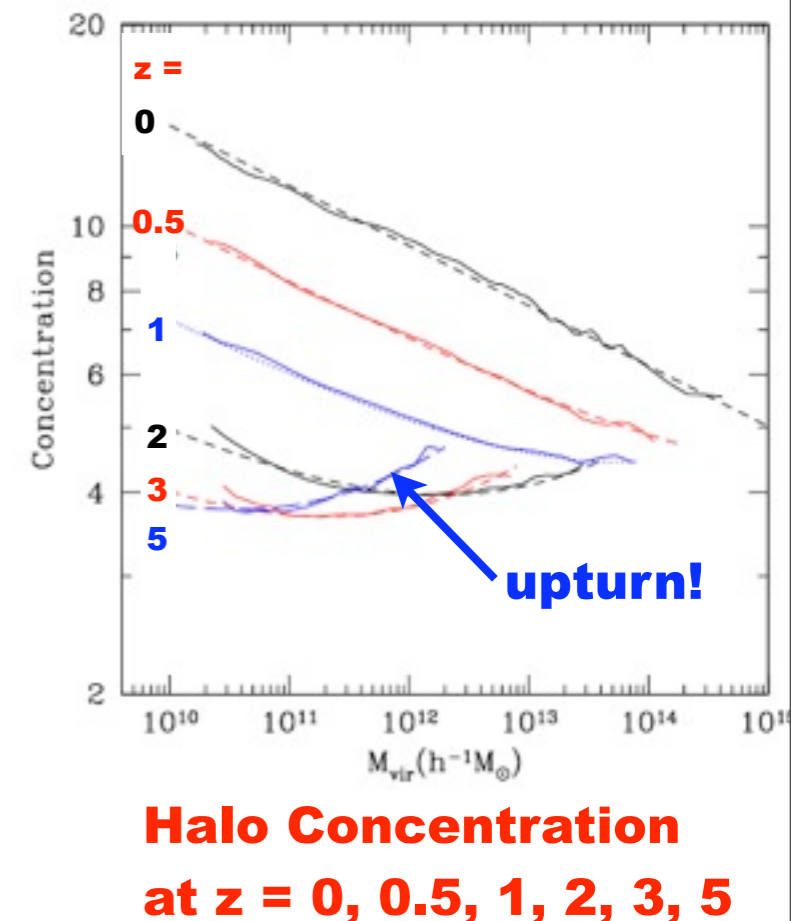
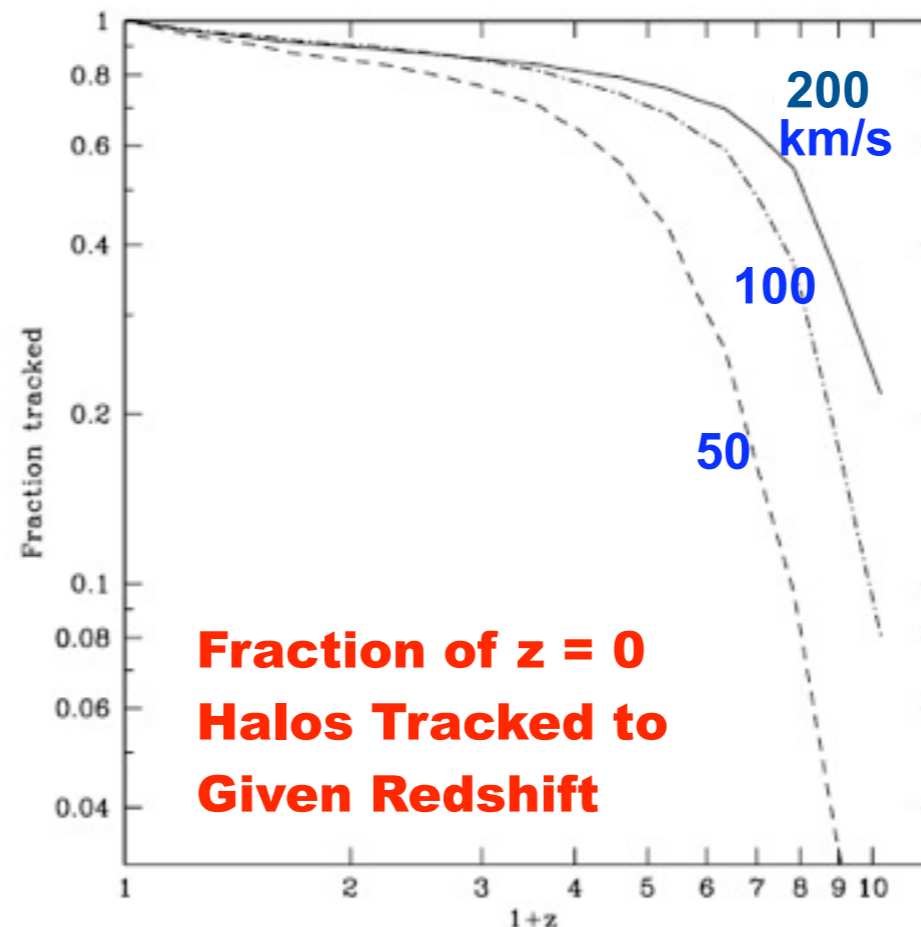
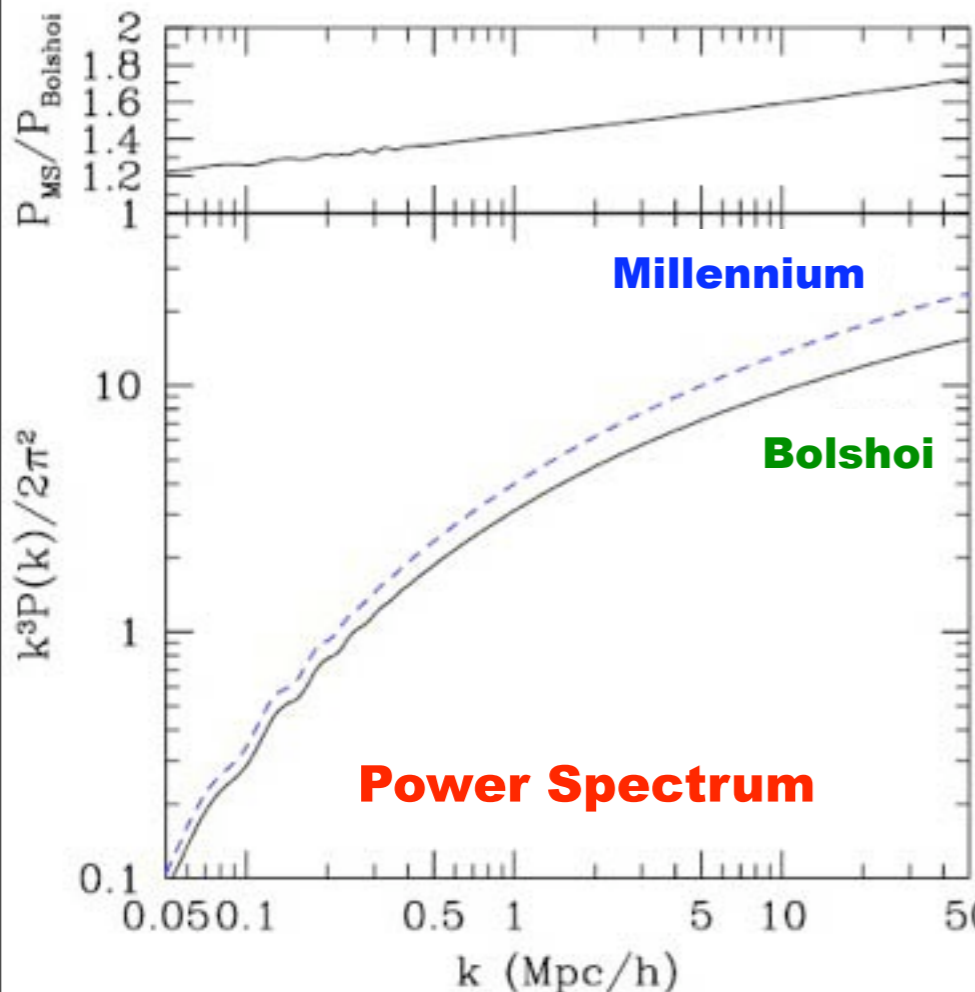
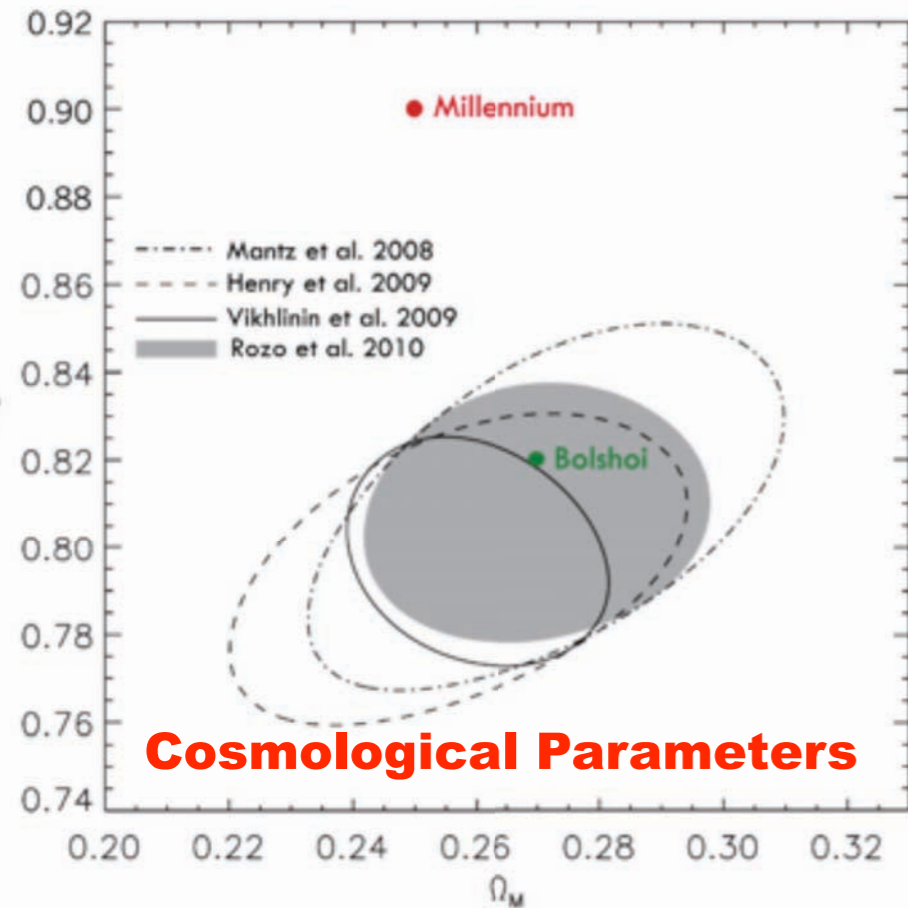
BOLSHOI SIMULATION FLY-THROUGH

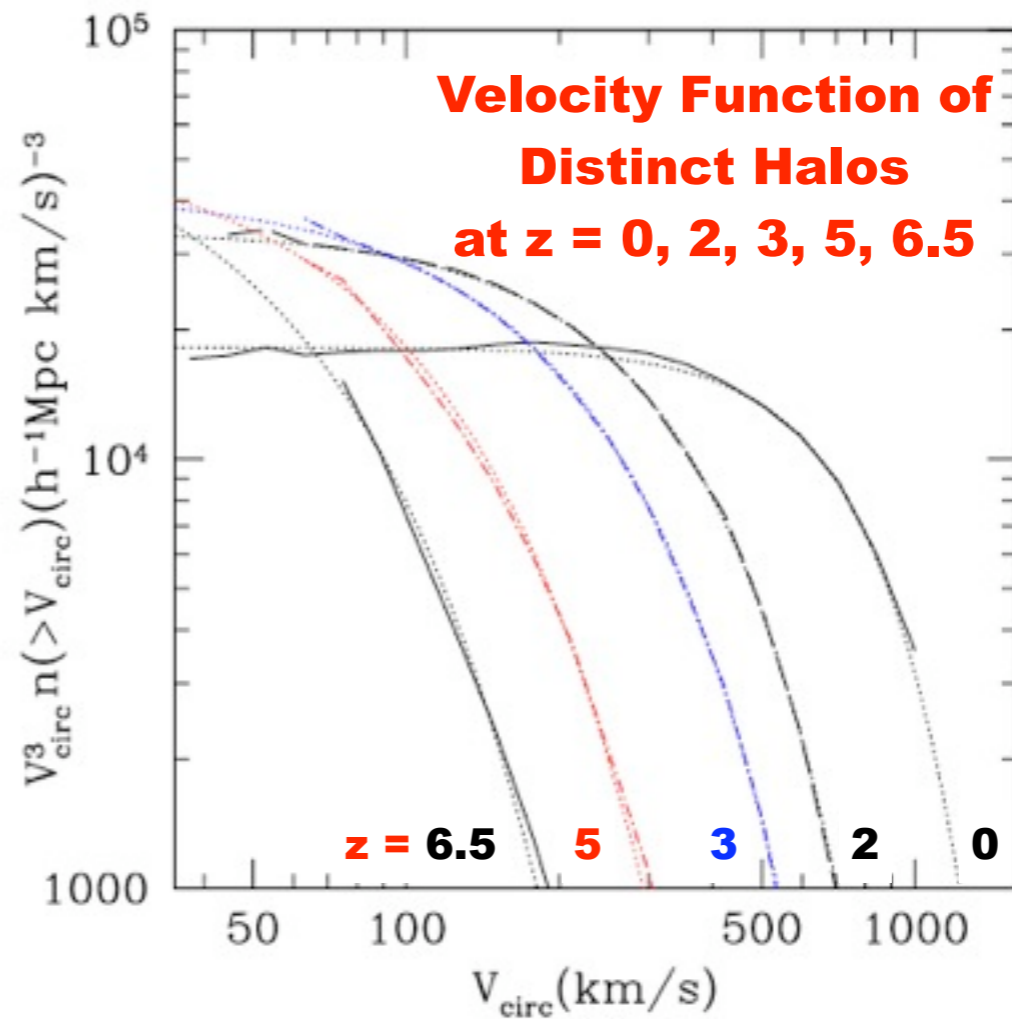
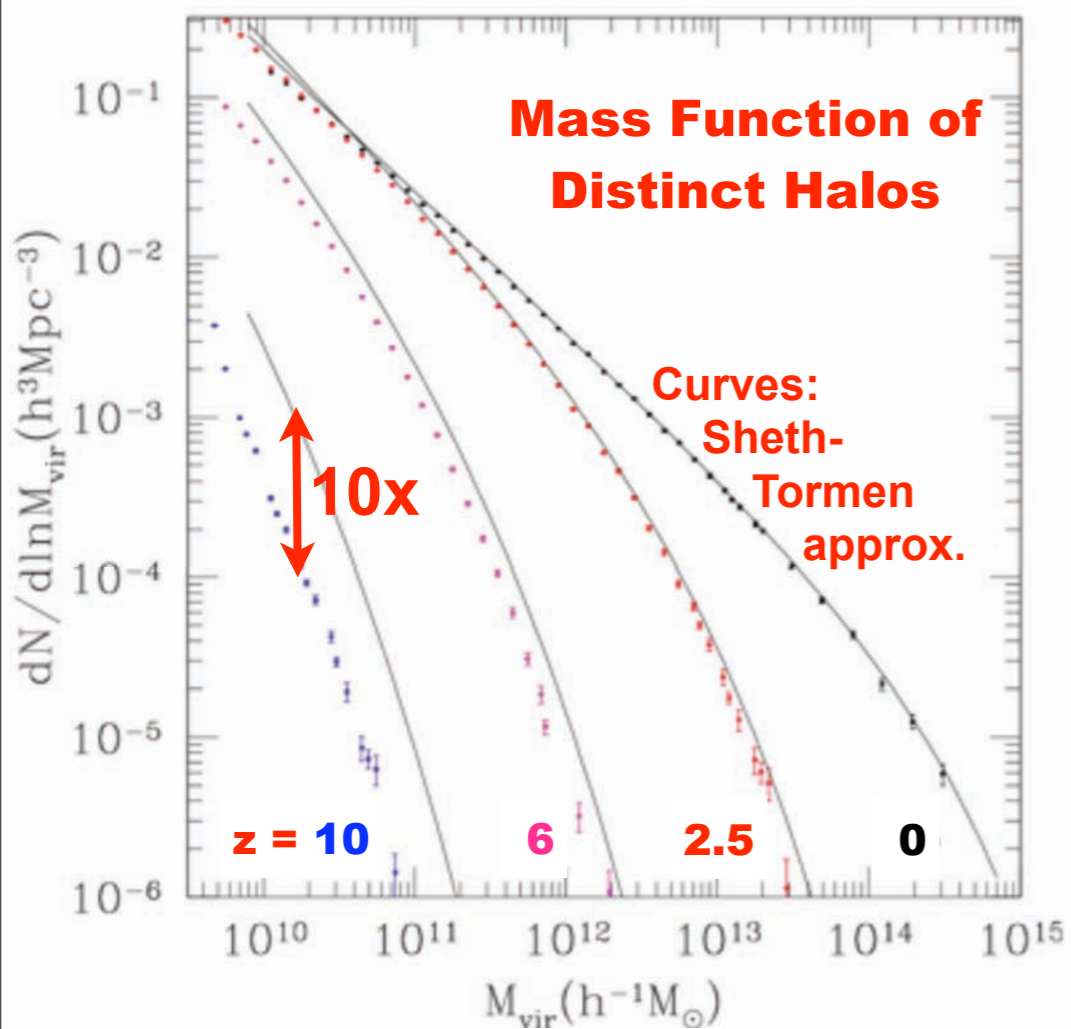


$<10^{-3}$
of the
Bolshoi
Simulation
Volume

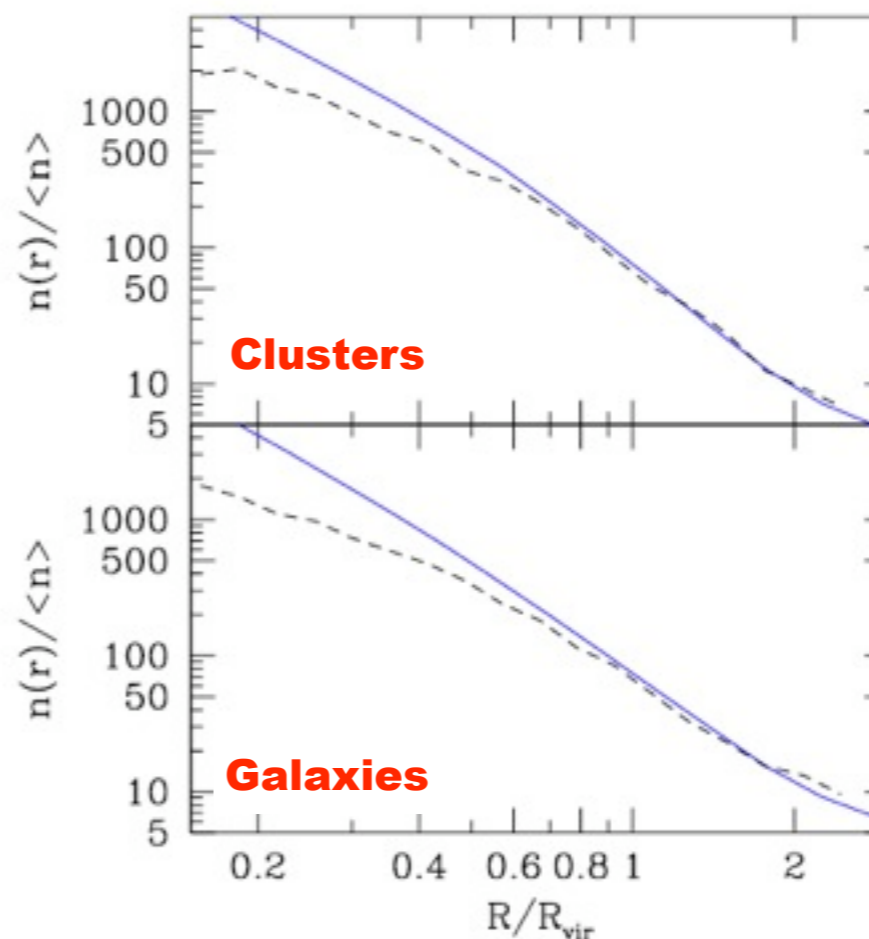
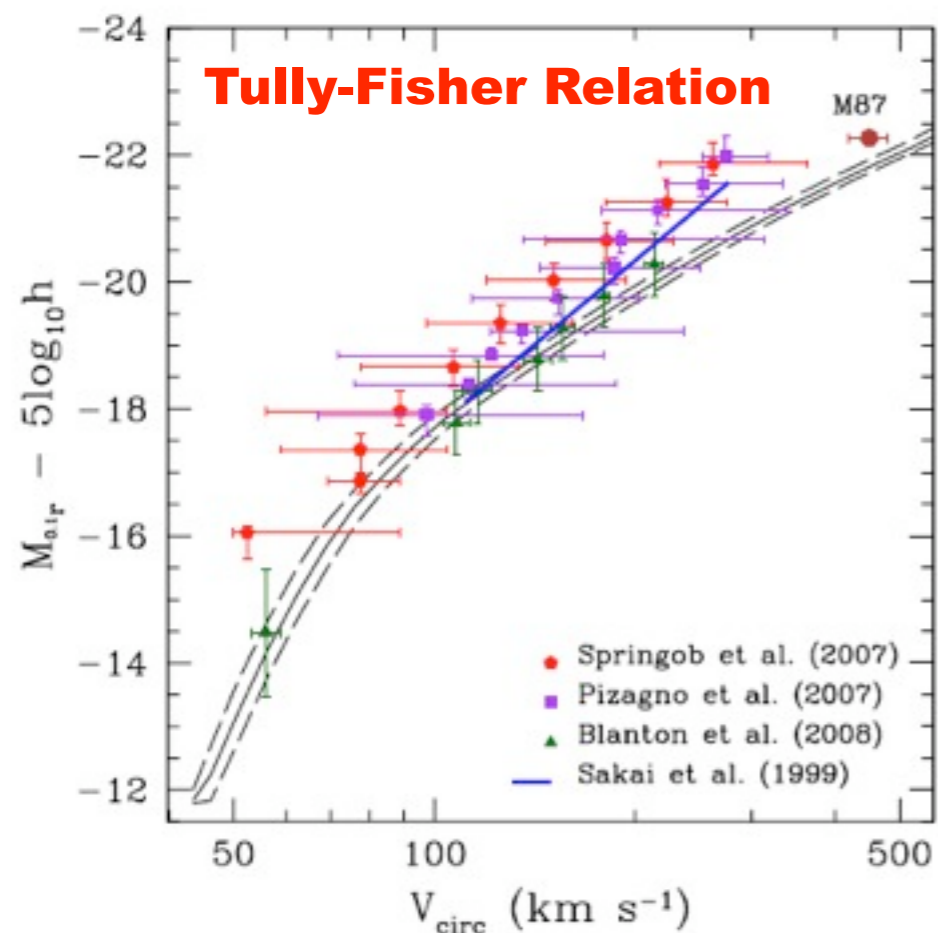
Halos and galaxies: results from the **Bolshoi** simulation

The **Millennium-I Run** (Springel+05) was a landmark simulation, and it has been the basis for ~300 papers. However, it and the new Millennium-II simulations were run using WMAP1 (2003) parameters, and the Millennium-I resolution was inadequate to see many subhalos. The new **Bolshoi** simulation (Klypin, Trujillo & Primack 2010) used the WMAP5 parameters (consistent with WMAP7) and has nearly an order of magnitude better mass and force resolution than Millennium-I. We have now found halos in all 180 stored timesteps, and we have complete merger trees. We are working with Darren Croton, Rachel Somerville, Lauren Porter and Andrew Benson on **semi-analytic models of the evolving galaxy population based on Bolshoi**, which should give better EBL predictions.

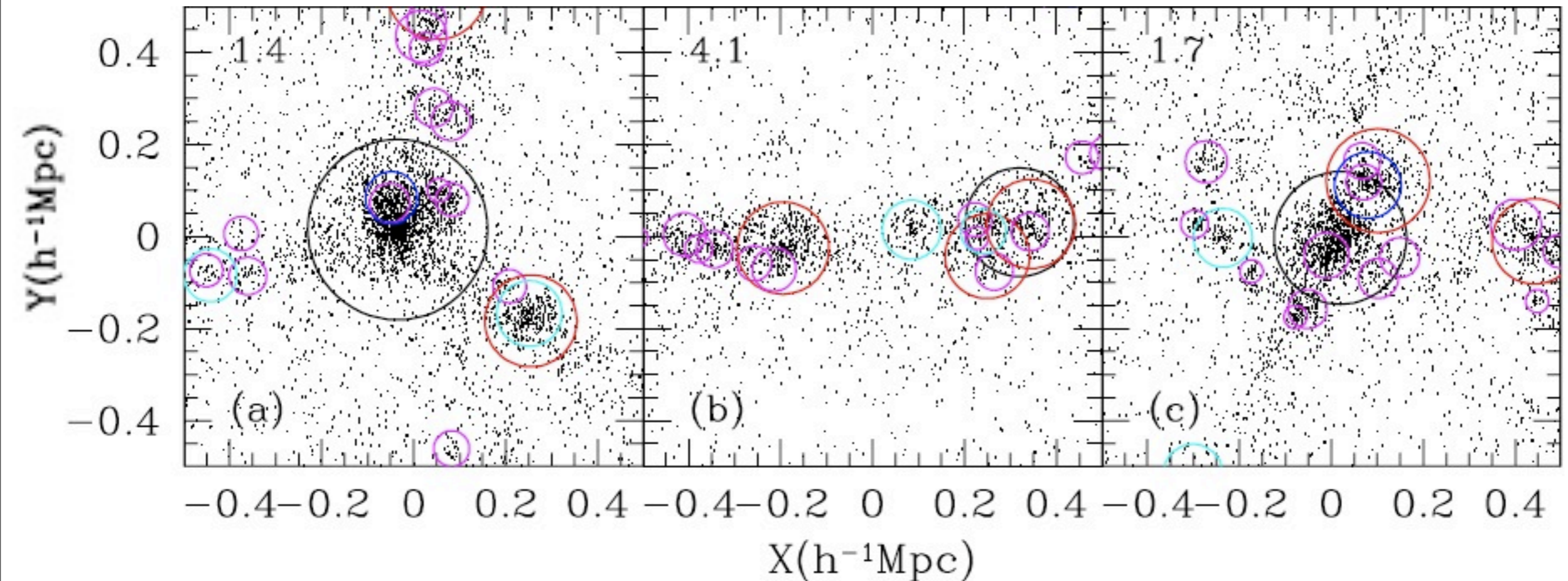




NOTE:
figures are from Klypin, Trujillo, & Primack, arXiv: 1002.3660



Subhalos follow the dark matter distribution except in the inner regions of cluster and galaxy halos



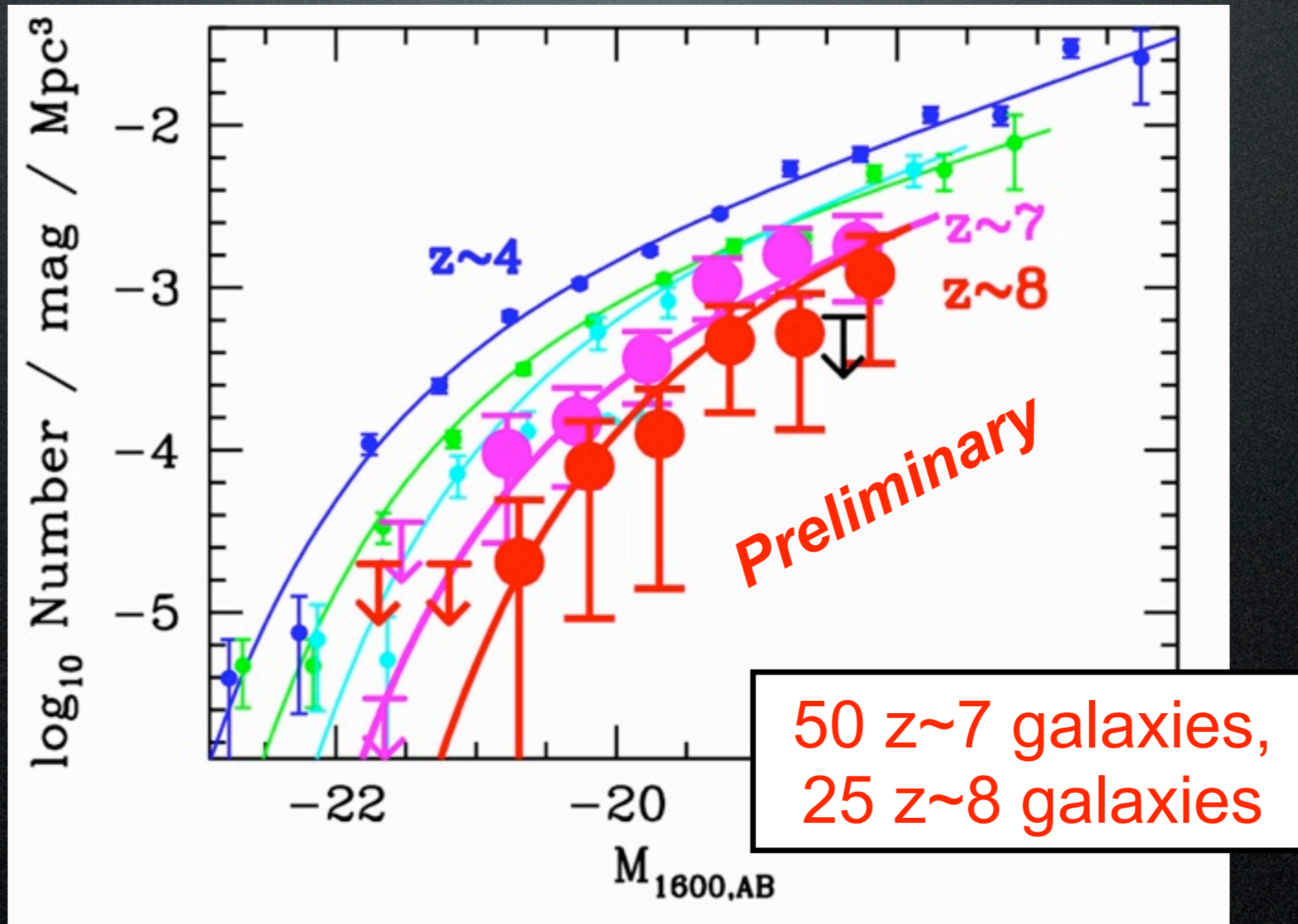
The distribution of mass around 3 massive halos ($M_{\text{FOF}} = 10^{11} h^{-1} M_{\text{sun}}$) at redshift $z = 8.8$. Each panel shows 1/2 of the dark matter particles in cubes of $1 h^{-1} \text{ Mpc}$ size. The center of each cube is the exact position of the center of mass of the corresponding FOF halo. The effective radius of each FOF halo in the plots is $150 - 200 h^{-1} \text{ kpc}$. Circles indicate distinct halos and subhalos identified by the spherical overdensity algorithm BDM. The radius of each circle is equal to the virial radius of the halo. In panel (b) FOF linked together a chain of halos which formed in long dense filaments. This happens often. The numbers in the top-left corner of each panel show the ratio of FOF mass to that of SO. **The Sheth-Tormen mass function agrees well with the abundance of halos with FOF masses, but these do not correspond to halos that will host forming galaxies as BDM halos do. Getting this right is important in understanding the new HST/WFC3 data on high-redshift galaxies, and also the reionization of the universe.**

Bolshoi simulation - Klypin, Trujillo & Primack 2010 - Appendix B

Wide area + Ultra-deep Observations can be used to more accurately constrain the UV LF at $z \sim 7-8$

UV Luminosity Functions

Log #
 mag^{-1}
 Mpc^{-3}



Bright

Faint

Bouwens et al. 2010

UCSC 02/01/10 RJB

Conclusions

Data from (non-)attenuation of gamma rays from AGN and GRBs gives upper limits on the EBL from UV to mid-IR that are $\sim 2x$ lower limits from observed galaxies. These upper limits now rule out some EBL models and purported observations, with improved data likely to provide even stronger constraints.

EBL calculations based on careful extrapolation from observations and on semi-analytic models are consistent with these lower limits and with the gamma-ray upper limit constraints.

Such comparisons “close the loop” on cosmological galaxy formation models, since they account for all the light, including that from galaxies too faint to see. They can constrain star formation models, including variations in the stellar initial mass function (IMF).